Title
Long wavelength light reduces the negative consequences of dim light at night.

Authors
Wang, Huei-Bin
Zhou, David
Luk, Shu
et al.

Publication Date
2023

DOI
10.1016/j.nbd.2022.105944

Peer reviewed

HHS Public Access

Author manuscript

Neurobiol Dis. Author manuscript; available in PMC 2023 October 24.

Published in final edited form as:

Neurobiol Dis. 2023 January ; 176: 105944. doi:10.1016/j.nbd.2022.105944.

Long wavelength light reduces the negative consequences of dim light at night

Huei-Bin Wang[a,b], **David Zhou**[b], **Shu Hon Christopher Luk**[b], **Hye In Cha**[b], **Amanda Mac**[b], **Rim Chae**[b], **Anna Matynia**[c], **Ben Harrison**[f], **Sina Afshari**[f], **Gene D. Block**[b], **Cristina A. Ghiani**[b,d,e], **Christopher S. Colwell**[b,e,*]

[a]Molecular, Cellular, Integrative Physiology Graduate Program, David Geffen School of Medicine, University of California Los Angeles, USA

[b]Department of Psychiatry & Biobehavioral Sciences, David Geffen School of Medicine, University of California Los Angeles, USA

[c]Laboratory of Ocular Molecular and Cellular Biology and Genetics, Jules Stein Eye Institute, David Geffen School of Medicine, University of California Los Angeles, USA

[d]Department of Pathology and Laboratory Medicine, David Geffen School of Medicine, University of California Los Angeles, USA

[e]Intellectual and Developmental Disabilities Center, David Geffen School of Medicine, University of California Los Angeles, USA

[f]Korrus Inc, Los Angeles, CA, USA

Abstract

Many patients with autism spectrum disorders (ASD) show disturbances in their sleep/wake cycles, and they may be particularly vulnerable to the impact of circadian disruptors. We have previously shown that a 2-weeks exposure to dim light at night (DLaN) disrupts diurnal rhythms, increases repetitive behaviors and reduces social interactions in contactin-associated protein-like 2 knock out (*Cntnap2* KO) mice. The deleterious effects of DLaN may be mediated by intrinsically photosensitive retinal ganglion cells (ipRGCs) expressing the photopigment melanopsin, which is maximally sensitive to blue light (480 nm). In this study, the usage of a light-emitting

*Corresponding author at: Laboratory of Circadian and Sleep Medicine, Department of Psychiatry & Biobehavioral Sciences, David Geffen School of Medicine, University of California Los Angeles, Los Angeles, CA 90024, USA. ccolwell@mednet.ucla.edu (C.S. Colwell).

Author contributions

HBW, GDB, CAG and CSC conceived the hypothesis and experimental design of this study. HBW, DZ, SHCL, HC, AM, RC performed the experiments and quantitative analyses. HBW, CAG and CSC analyzed the data. HBW DSW wrote for the first draft, CAG and CSC edited, wrote and compiled the final version paper with contribution from the other authors.

Disclosures

The authors of this work have no financial interests directly related to this manuscript. Ben Harrison and Sina Afshari are employed by Korrus Inc. and have a financial interest in the commercial use of the LED lighting system for humans.

Data sharing

Available from the corresponding author upon request.

Appendix A. Supplementary data

Supplementary data to this article can be found online at https://doi.org/10.1016/j.nbd.2022.105944.

diode array enabled us to shift the spectral properties of the DLaN while keeping the intensity of the illumination at 10 lx. First, we confirmed that the short-wavelength enriched lighting produced strong acute suppression of locomotor activity (masking), robust light-induced phase shifts, and cFos expression in the suprachiasmatic nucleus in wild-type (WT) mice, while the long-wavelength enriched lighting evoked much weaker responses. *Opn4*^{DTA} mice, lacking the melanopsin expressing ipRGCs, were resistant to DLaN effects. Importantly, shifting the DLaN stimulus to longer wavelengths mitigated the negative impact on the activity rhythms and 'autistic' behaviors (i.e. reciprocal social interactions, repetitive grooming) in the *Cntnap2* KO as well as in WT mice. The short-, but not the long-wavelength enriched, DLaN triggered cFos expression in in the basolateral amygdala (BLA) as well as in the peri-habenula region raising that possibility that these cell populations may mediate the effects. Broadly, our findings are consistent with the recommendation that spectral properties of light at night should be considered to optimize health in neurotypical as well as vulnerable populations.

Keywords

Autism spectrum disorder; Amygdala; cFos; Circadian; *Cntnap2* knock out; Light pollution; Melanopsin; Mice

1. Introduction

Dim light at night (DLaN) is a common environmental perturbation of the circadian timing system and has been linked to a range of deleterious consequences (Stevenson et al., 2015; Lunn et al., 2017). Prior work in pre-clinical models has demonstrated that light at night negatively impacts the metabolism (Fonken et al., 2013a; Plano et al., 2017), immune function (Bedrosian et al., 2011; Fonken et al., 2013b; Lucassen et al., 2016), mood and cognition (Lazzerini Ospri et al., 2017; An et al., 2020; Walker 2nd et al., 2020). Individuals diagnosed with autism spectrum disorders (ASD) commonly experience disturbances in their circadian rhythms, and find difficulty in both falling asleep as well as sleeping through the night (Cohen et al., 2014; Devnani and Hegde, 2015; Mazurek and Sohl, 2016; Baker and Richdale, 2017; Shelton and Malow, 2021). Perhaps, because of the difficulty sleeping, ASD patients spend more time exposed to electronic screens at night compared with age-matched controls (Engelhardt et al., 2013; Mazurek et al., 2016; Stiller et al., 2019; Healy et al., 2020; Dong et al., 2021). It has been speculated that exposure to DLaN via screens and other lighting sources could be detrimental to ASD populations. In support of this speculation, we previously reported that an animal model carrying a genetic risk factor associated with ASD (contactin associated protein-like 2, *Cntnap2*) shows reduced social preference and increased stereotypic grooming behavior after a 2-week exposure to DLaN (Wang et al., 2020).

The negative effects of nightly light exposure could be mediated by the intrinsically photosensitive retinal ganglion cells (ipRGCs) expressing the photopigment melanopsin, which is maximally sensitive to shorter wavelengths (λ) of light with a peak response to 480 nm light (Hattar et al., 2002; Panda et al., 2005). ipRGCs receive inputs from rod and cone photoreceptors (Hattar et al., 2002; Dacey et al., 2005; Lucas et al., 2012; Van Diepen et al., 2021) with the rods driving the circadian response to low-intensity light (Altimus et

al., 2010; Lall et al., 2010). These findings indicate that the circadian system is sensitive to a broad spectrum of light (Foster et al., 2020), and raise the question if changes in the spectral properties of DLaN matter. Perhaps the intensity of the night-time illumination is the only parameter biologically important? Recent studies are beginning to address the issue of whether adjusting the spectral composition of light to reduce melanopic stimulation can be used as a strategy to minimize disruption of circadian rhythms (Gladanac et al., 2019; Nagare et al., 2019a, 2019b; Figueiro and Pedler, 2020; Mouland et al., 2021; Vethe et al., 2021).

In the present study, we employed an array of light-emitting diodes (LEDs) to generate dim illumination (10 lx) with a spectral composition enriched in either shorter wavelengths (λ), designed to activate melanopsin, or longer λ to minimize activation of this photopigment. First, we ascertained in wild-type (WT) mice whether the two light treatments differentially regulated negative masking behavior, light-induced phase shifts of circadian behavior as well as the light-evoked cFos response in the suprachiasmatic nucleus (SCN). A transgenic line of mice (*Opn4*^{DTA}) lacking melanopsin and with diminished ipRGCs due to the targeted expression of diphtheria toxin A in the *Opn4* expressing cells (Matynia et al., 2012; Chew et al., 2017) was used to evaluate the contribution of the ipRGCs in mediating the effects of DLaN. Next, we determined whether the two light treatments differentially impacted DLaN-driven changes in daily patterns of activity, sociability, and grooming in WT and *Cntnap2* knock-out (KO) mice. Finally, we examined whether short-λ enhanced DLaN altered light-evoked changes in the number of cFos positive cells in selected brain regions in both WT and *Cntnap2* KO mice.

2. Materials and methods

2.1. Animals

All animal procedures were performed in accordance with the UCLA animal care committee's regulations. Both adult male and female mice (3–4 months old, mo) were used in this study. *Cntnap*^{2tm2Pel}/J mutant mice backcrossed to the C57BL/6 J background strain (B6.129(Cg)-*Cntnap2tm2Pele*/J, stock number 017482; RRID:IMSR_JAX:017482) and the control C57BL/6 J strain (stock number 000664; RRID: IMSR_JAX:000664) were from our breeding colony maintained in an approved facility of the Division of Laboratory Animal Medicine at the University of California, Los Angeles (UCLA). WT and *Cntnap2* KO mice were obtained from heterozygous breeding pairs, weaned at postnatal day 21 and genotyped (TransnetYX, Cordova, TN). *Opn4*^{DTA} mice (*Opn4*$^{tm3.1(DTA)Saha}$/J; stock number 035927; RRID:IMSR_JAX:035927) and their WT littermates were kindly provided by Dr. Anna Matynia (Jules Stein Eye Institute, UCLA). *Opn4*^{DTA} mice backcrossed into the C57Bl/6 J background express the diphtheria toxin subunit alpha (DTA) sequence under the control of the Opn4 promoter (exons 1–9 of the opsin 4) resulting in the ablation of the ipRGCs. These mice were bred heterozygous to heterozygous and ipRGC ablation was verified using a qualitative Pupillary Light Reflex assay as reported (Matynia et al., 2012). Vglut2-ires-Cre knock-in mice (B6J.129S6(FVB)-Slc17a6$^{tm2(cre)Lowl}$/MwarJ; stock number 028863; RRID:IMSR_JAX:028863) carrying a Cre recombinase targeting excitatory glutamatergic neurons, as well as Ai6 mice (B6.Cg-Gt(ROSA)26Sor$^{tm6(CAG-ZsGreen1)Hze}$/J;

stock number 007906; RRID:IMSR_JAX:007906) expressing robust ZsGreen1 fluorescence following Cre-mediated recombination were obtained from Jackson Laboratory. The Ai6 is a Cre reporter allele designed to have a loxP-flanked STOP cassette preventing transcription of a CAG promoter-driven enhanced green fluorescent protein variant (ZsGreen1) - all inserted into the Gt(ROSA)26Sor locus. We bred this floxed reporter gene into the Cntnap2 mutant to create *Cntnap2* KO mice heterozygous for Vglut2 Cre-Ai6 (ZsGreen1). Cohorts of male and female mice were group housed prior to experimentation.

2.2. Lighting manipulations

Mice were housed in light-tight ventilated cabinets in temperature- and humidity-controlled conditions, with free access to food and water. All the mice were first entrained to a normal lighting cycle: 12:12 h light: dark (LD). Light intensity during the day was 300 lx as measured at the base of the cage, and 0 lx during the night. The time of lights-on defines Zeitgeber Time (ZT) 0 and the time of lights-off defines ZT 12. Following entrainment to normal LD, mice were singly housed under three different lighting conditions for 2 weeks: (1) LD, (2) night light with a spectral composition aimed at minimizing melanopsin stimulation (long λ-enriched lights) or (3) at maximizing melanopsin stimulation (short λ-enriched lights). The treated mice were exposed nightly to one of these light conditions from ZT 12 to 24. The short- and long-wavelength (10 lx intensity) were generated by the Korrus Inc. (Los Angeles, CA) LED lighting system (S. Fig. 1). Following recent recommendations (Lucas et al., 2014), the LED output was measured with an UPRtek spectrophotometer (Model MK350S, Taiwan) at the level of the cage floor. Using the International Commission on Illumination (CIE) S 026 α-opic Toolbox (DOI: 10.25039/S026.2018), the melanopic α-opic irradiance of the long-λ enhanced and the short-λ enhanced output was estimated to be at 0.001 W/m^2 and 0.020 W/m^2, respectively. The melanopic α-opic equivalent daylight (D65) illuminance of the long-λ output was estimated at 1 melanopic lx, and the short-λ output at 15 melanopic lx. The total energy of the long-λ enhanced light was measured as an illumination of 10.4 lx, irradiance of 0.05 W/m^2, log photon irradiance of 17.2 s^1/m^2, and for the short-λ enhanced light as an illumination of 10.0 lx, irradiance of 0.03 W/m^2, log photon irradiance of 17.0 s^1/m^2. One simple way of comparing light sources is the M/P ratio (melanopic lx divided by photopic lx). For daylight, this will be 1. In our study, the M/P was 1.49 for the short-λ illumination and 0.11 for the long-λ illumination.

Daily pattern of activity was monitored using a top-mounted passive infra-red (IR) motion detector reporting to a VitalView data recording system (Mini Mitter, Bend, OR) as previously described (Wang et al., 2017, 2018). Detected movements were recorded in 3 min bins, and 10 days of data were averaged for analysis using the El Temps chronobiology program (A. Diez-Noguera, Barcelona, Spain; http://www.el-temps.com/principal.html). The strength of the rhythm was determined from the amplitude of the χ^2 periodogram at 24 h, to produce the rhythm power (%V) normalized to the number of data points examined. The periodogram analysis uses a χ^2 test with a threshold of 0.001 significance, from which the amplitude of the periodicities is determined at the circadian harmonic to obtain the rhythm power. The percentage of sleep-phase activity was determined by the relative distribution of activity during the day versus the night. Fragmentation and onset variability were determined using the Clocklab program (Actimetrics, Wilmette, IL; http://actimetrics.com/

products/clocklab/). Fragmentation was determined by the number of activity bouts. Each bout was counted when activity bouts were separated by a gap of 21 min. The onset variability was calculated by first determining the daily onset of activity over 10 days, and then the deviation from the best-fit line drawn through the 10 onset times. To produce the representative waveforms, hourly running averages of the same series of activity data were plotted against time of day.

2.3. Photic suppression of nocturnal activity (negative light masking)

A separate cohort of WT mice (3–4 mo) were individually housed in cages with IR motion detector in light-tight chambers under a 12:12 LD cycle to determine the effects of LED lights (Korrus Inc) at night on masking of nocturnal activity. Their locomotor activity was recorded per 3-min interval and monitored to ensure the entrainment to the housing LD cycles. The animals were exposed to light (enriched for long- or short-λ) for 1 h at ZT 14. The activity level during the light exposure was compared to the activity level during the equivalent time (ZT 14 to 15) on the day before the treatment.

2.4. Phase shift of activity rhythms

After habituation to running wheel cages, a different cohort of WT mice (3–4 mo) was released into constant darkness (DD) for 10 days. The circadian time (CT) of their free-running sleep/wake cycles was monitored with the VitalView. The time of activity onset under DD was defined as CT 12. On day 11, the mice were exposed to long- or short-λ light (10 lx, 60 min) at CT 16 for 15 min, after the treatment, the mice were held in DD for the subsequent 10 days. The best-fit lines of the activity onsets of the sleep/wake cycles before and after the treatment were determined and compared.

2.5. Photic induction of cFos in the SCN and immunofluorescence

A separate cohort of WT mice (3–4 mo) was housed in DD conditions (Wang et al., 2017), and exposed to normal white light, long- or short-λ light (10 lx) for 15 mins at CT 16. Forty-five mins later, the mice were euthanized with isoflurane (30%–32%) and transcardially perfused with phosphate-buffered saline (PBS, 0.1 M, pH 7.4) containing 4% (*w*/*v*) paraformaldehyde (Sigma). The brains were rapidly dissected out, post-fixed overnight in 4% PFA at 4 °C, and cryoprotected in 15% sucrose. Sequential coronal sections (50 μm), containing the middle SCN, were collected using a cryostat (Leica, Buffalo Grove, IL) and further processed for cFos immunofluorescence as reported below.

2.6. Behavioral tests

The reciprocal social interaction test was used to assess general sociability and interest in social novelty. On the days of testing, the animals were taken out from the light-tight chambers and habituated to the testing room for at least 30 mins. To avoid sleep disruptions, all behavioral tests were conducted in the middle of the dark phase (ZT 16–18). The social behavior was evaluated by first familiarizing the testing mouse with the testing arena first (habituation for 30 mins), and then by introducing a never-met stranger mouse into the same arena. The stranger mouse was same age, sex, and genotype as the testing mouse. The two mice were allowed to interact for 10 mins, and the testing trials were recorded by

a camcorder. Duration of sniffing (nose to nose sniff and nose to anogenital sniff), social grooming (the testing mouse grooms the novel stranger mouse on any part of the body) and touching was assessed and reported for the time of social behavior.

The grooming test (Wang et al., 2020) was performed to evaluate the level of the animals' stereotypic behavior (ZT 16–18). After the habituation to the testing room for at least 30 mins, the mice were introduced to the testing arena and their behavior was recorded by a camcorder for 30 mins.

2.7. Immunofluorescence

At the end of the 2-weeks exposure to the 3 different lighting conditions, mice were anesthetized with isoflurane at a specific time during the night (ZT 18) and transcardially perfused with phosphate buffered saline (PBS, 0.1 M, pH 7.4) containing 4% (*w*/*v*) paraformaldehyde (Sigma). The brains were rapidly dissected out, post-fixed overnight in 4% PFA at 4 °C, and cryoprotected in 15% sucrose. Coronal sections (50 μm) were obtained using a cryostat (Leica, Buffalo Grove, IL), collected sequentially, and paired along the anterior–posterior axis before further processing. Immunohistochemistry was performed as previously described (Wang et al., 2017; Lee et al., 2018). Briefly, free-floating coronal sections containing the brain regions of interest were blocked for 1 h at room temperature (1% BSA, 0.3% Triton X-100, 10% normal donkey serum in 1xPBS) and then incubated overnight at 4 °C with a rabbit polyclonal antiserum against cFos (1:1000, Millipore or Cell Signaling) followed by a Cy3-conjugated donkey-anti-rabbit secondary antibody (Jackson ImmunoResearch Laboratories, Bar Harbor, ME). Sections were mounted and coverslips applied with Vectashield mounting medium containing DAPI (4′−6-diamidino-2-phenylinodole; Vector Laboratories, Burlingame, CA), and visualized on a Zeiss AxioImager M2 microscope (Zeiss, Thornwood NY) equipped with an AxioCam MRm and the ApoTome imaging system.

2.8. cFos positive cell counting

Images for counting were acquired using either a 20× or 40× objective and the Zeiss Zen digital imaging software. Both male and female mice, in equal number, were used for each assessment and two observers masked to genotype and experimental group performed the cell counting.

Photic induction of cFos in the SCN: Images of both the left and right middle SCN were acquired with a 20× objective using the tile tool of the Zen software. The SCN was manually traced in each image using the NIH ImageJ software (https://imagej.net/software/fiji/), and the cells immunopositive for cFos counted with the aid of the cell counter plugin of ImageJ in two consecutive sections at the level of the mid-SCN. Values from the left and right SCN in the two slices were averaged to obtain one value per animal and are presented as the mean ± SEM of 4 animals/experimental group.

cFos expression in different brain regions of interest: Images of all the regions of interest (both right and left hemisphere) were acquired with a 20× objective using the tile tool of the Zen software. Each brain area was manually traced to define the regions

of interest and all the cells immunopositive for cFos were counted with the aid of the cell counter plugin of ImageJ in two consecutive sections. Values from the left and right hemispheres in the two slices were averaged to obtain one value per animal and are presented as the mean ± SEM of 6 animals/genotype/experimental group.

cFos expression in the Basolateral Amygdala of vGlut2-ZsGreen1 expressing mice: Seven to fifteen images from the left and right Basolateral Amygdala (BLA) were randomly acquired with a 40× objective from 6 consecutive slices/animal. Two investigators masked to genotype and treatment group performed the cell counting using the Zen software tools in 5–7 images/animal. The followings were quantified in each image: (1) the total number of vGlut-ZsGreen1 cells; (2) the number of vGlut-ZsGreen1 cells immunopositive for cFos. The percentage of cFos positive cells/vGlut-ZsGreen1 cells per image was determined and then averaged to obtain a single value/animal. On average, each image contained about 30–45 vGlut-ZsGreen1 cells, with the *Cntnap2* KO exposed to short-λ enriched DLaN having the lowest counts (about 33 cells). Data are shown as the mean ± SEM of 4 animals/genotype/experimental group, 2 males and 2 females were present in each group.

2.9. Statistics

SigmaPlot (version 12.5, SYSTAT Software, San Jose, CA) or GraphPad Prism (version 9.4.1, GraphPad Software, San Diego, CA) was used to run statistical analyses. Cohorts of mice kept in LD are referred to as LD controls. One-way analysis of variance (ANOVA) was used to determine the significance of the impact of light exposure on the three assays for the light input to the circadian system in WT mice (Fig. 1). Two-way ANOVA was used to analyse (1) the waveforms of the activity rhythms with time and treatment as factors (Fig. 2; S. Fig. 2; S. Fig. 4; S. Fig. 5); (2) other parameters of the activity rhythms and other behavioral tests (Figs. 2, 4) with genotype and treatment as factors; (3) the number of cFos positive cells in different brain regions with genotype and treatment as factors (Fig. 5, S. Fig. 6); (4) sex differences with sex and genotype as factors (S. Figs. 4, 5). The Holm-Sidak test for multiple comparisons was used when appropriate. Finally, a paired-*t*-test was used when comparing behavioral data in the same subject before and after light exposure (Fig. 3, S. Fig. 3), regardless of the genotype. This test offers a sensitive tool to evaluate the impact of the treatment in the same animal regardless of the genotype and address animal variability in responses to the different lighting. Values are reported as the mean ± standard error of the mean (SEM). Differences were determined significant if $P < 0.05$.

3. Results

3.1. Long-λ enriched illumination reduces negative masking, light-induced phase shifts of the circadian activity rhythm, and cFos induction in the SCN through a pathway dependent upon Opn4 expressing neurons

In these first set of control experiments, we tested the hypothesis that long-λ enhanced lighting would evoke a reduced response on three classic tests of the ipRGC input to the circadian system in WT mice. The effects on light-driven suppression or “masking” of activity were measured with a passive infra-red activity assay while mice were held in an LD

cycle. The short-λ enriched light (10 lx, 60 min, at ZT 14) elicited a significant reduction (51 ± 5%) in locomotor behavior in the WT that was comparable to the response to white light (51 ± 5%) (Fig. 1A, Table 1). In contrast, the long-λ illumination produced a much lower suppression of activity (14 ± 7%), which was not significantly different from the untreated controls. Next, we measured the impact of the two treatments on the light-induced phase shift of the circadian system using wheel-running activity. WT mice, held in DD, were exposed to short- or long-λ lighting (10 lx, 15 min, at CT 16) and free-running locomotor activity rhythms measured. The short-λ light triggered a phase delay (−117 ± 6 min) in the mice comparable to the phase delay evoked by white light (−128 ± 12 min), whilst the response to the long-λ (−26 ± 4 min) was not significantly different as compared to untreated controls (Fig. 1B, C; Table 1). The effect of a 15 min light pulse (10 lx) with one of the three lightings, given 4 h after the onset of activity (CT 16) to mice held in DD, was evaluated on the number of cFos immunopositive cells in the SCN. The mice exposed to the short-λ light exhibited a robust induction of cFos (94 ± 6 cells per animal) in the SCN comparable to that elicited by white light (85 ± 6). Whilst WT that received a pulse with the long-λ light had significantly fewer immunopositive cells (Fig. 1D,E; Table 1). Hence, shifting the spectral properties of light toward longer wavelengths significantly reduced the effects of light on the master regulator of the circadian system, the SCN.

As an additional control, we utilized a line of mice ($Opn4^{DTA}$) with reduced numbers of ipRGCs due to the targeted expression of the diphtheria toxin A in the Opn4 expressing cells (Matynia et al., 2012; Chew et al., 2017). $Opn4^{DTA}$ mice and their WT littermates were held under either LD (control environment) or exposed to the short-λ enriched DLaN for 2 weeks. The WT mice exposed to the short-λ enriched DLaN exhibited a robust reduction in the strength of the activity rhythms (activity levels, power, amplitude), but these parameters were unaltered in the mutants (S. Fig. 2A,B; Table 2). Next, we examined acute light suppression of activity in mice of both genotypes held in LD and exposed to one of the two lights for 60 min at CT 14. Again, while the WT mice exhibited a drastic suppression of their activity (42 ± 7%), the $Opn4^{DTA}$ did not show any light-evoked change in their activity (9 ± 9%; S. Fig. 2C; Table 2). Together these data indicate that the ipRGCs are required for at least some of the detrimental effects of DLaN.

3.2. Reduced melanopic illumination prevents DLaN-driven disruption of daily rhythms in activity in WT and Cntnap2 KO mice

Exposure to DLaN for 2 weeks greatly impacts the locomotor activity rhythms in both WT mice and *Cntnap2 KO* mice (Wang et al., 2020), thus, we tested the hypothesis that exposure to long-λ enriched illumination would reduce this effect on behavior. Cohorts of WT and *Cntnap2* KO mice were first housed under control conditions (LD 12:12), then randomly exposed to either long- or short-λ enriched DLaN (10 lx) for 2 weeks (Fig. 2A). Under LD conditions, both WT and *Cntnap2* KO mice exhibited robust rhythms in activity, although several parameters (total activity, power, amplitude) measured from the *Cntnap2* KO mice were consistent with weaker rhythms as previously described (Wang et al., 2020). When treated with the short-λ enriched DLaN, the average waveform (1 h bins) of both genotypes was significantly altered (Fig. 2A, B; Table 3), and both genotypes exhibited a significant reduction in several activity rhythm parameters (Fig. 2C–G; Table 3). Conversely,

the long-λ enriched illumination did not produce significant changes compared to LD (Fig. 2A–G; Table 3). These differences in the effects of the short- and long-λ illumination were strikingly evident when some of the key activity parameters were examined in each animal before and after light exposure (Fig. 3). For this purpose, we used a paired *t*-test as a sensitive measure to better visualize variability in the response to each illumination. These results strongly suggest that the spectral properties of the light used for illumination play a significant role in the adverse effects elicited by DLaN in both WT and *Cntnap2* KO mice.

3.3. Reduced melanopic illumination prevents DLaN-driven disruption of social behavior in WT and Cntnap2 KO mice as well as repetitive behavior in mutant mice

DLaN significantly impairs social behavior in both WT and *Cntnap2* KO (Wang et al., 2020), thus, we investigated if the long-λ enriched illumination would be less disruptive in a reciprocal social interaction test. The short-λ enriched DLaN treatment significantly decreased social behavior in both *Cntnap2* KO and WT mice, while the long-λ enriched light was without effect (Fig. 4A; Table 3). Further analyses of the social behavior of individual mice before and after exposure, showed that the short-λ DLaN decreased social interactions (>10%) in the majority of the mutant mice (10 out of the 12), whereas the long-λ DLaN affected social interactions in fewer KO mice (5 out of 12; S. Fig. 3A). Our findings indicate that exposure to short-λ enriched DLaN disrupted social behavior in both genotypes, and the use of longer λ illumination could effectively lessen the impact of DLaN on social behavior.

We have previously shown that *Cntnap2* KO, but not WT, mice exposed to DLaN display increased grooming, a measure of repetitive behavior (Wang et al., 2020). Hence, we posited that the long-λ enriched illumination would have a reduced effect on the DLaN-evoked increase in repetitive behavior. As previously observed, the *Cntnap2* KO mice exhibited higher levels of grooming than WT mice under normal LD conditions, which were further increased by exposure to the short-λ enriched DLaN, but unaffected by the long-λ enriched DLaN (Fig. 4B, Table 3). Neither light treatment altered the levels of grooming in the WT. Importantly, as shown in S. Fig. 3B, the short-λ enriched DLaN treatment triggered a selective increase in the time of grooming in the majority of the *Cntnap2* KO mice (Table 3) in the majority of the mutants (>10%; 16 out of the 22 KO). Conversely, only 4 mutants displayed an increase in grooming when exposed to the long-λ DLaN (Fig. 6C). Our observations demonstrate that the impact of DLaN on a measure of repetitive behavior in the *Cntnap2* KO was dependent upon the λ used.

3.4. Limited sex differences in the DLaN-driven behavioral changes in WT and Cntnap2 KO mice

Given the strong male bias in the prevalence of ASD, we powered our behavioral studies to test the hypothesis that males would be more impacted than females. First, we compared key measures of activity rhythms, social interactions and grooming between the two genotypes in mice held in normal LD conditions. Most of the activity rhythm parameters were not influenced by sex (Table 4) with the *Cntnap2* KO showing hypo-activity throughout the night. As previously described, the activity waveforms were more robust in the WT females compared to males, with higher activity levels in the early night (S. Fig. 4). We

found a similar situation for the social behavior, where there were significant effects of genotype but not sex (S. Fig. 4B; Table 4). In contrast, differences in the grooming behavior were influenced by both genotype and sex, with the mutants showing significantly altered measures of repetitive behavior and the male mutants showing a worse phenotype (S. Fig. 4C; Table 4). When these same parameters were compared in male and female WT and *Cntnap2* KO mice held under short-λ enriched DLaN conditions, no significant sex differences were found in any of the behaviors. For activity measures, there were not even differences between the genotypes as all of the rhythms were compromised (S. Fig. 5A; Table 5). Social interactions and grooming were compromised in both sexes, albeit more pronounced in the mutant mice (S. Fig. 5B,C; Table 5). In short, although we powered our sample size to detect possible sex differences, for the most part, both sexes were impacted by the *Cntnap2* mutation.

3.5. Reduced melanopic illumination diminished DLaN induction of cFos in the basolateral amygdala in Cntnap2 KO mice

Prior work has shown that activation of the ipRGC can drive cFos expression in several brain regions including the hypothalamus and the limbic system (Milosavljevic et al., 2016; Fernandez et al., 2018). Hence, we sought to test the hypothesis that 2 weeks exposure to DLaN would trigger cFos immunoreactivity in brain regions implicated in the control of repetitive behavior, such as the BLA, the Periventricular Nucleus (PVN), and the Lateral Hypothalamus (LH). We also examined possible DLaN-driven cFos expression in two areas known to receive light information from ipRGC, the SCN and peri-Habenular nucleus (pHb). Compared to mice held on a standard LD cycle, WT and *Cntnap2* KO mice exposed for 2 weeks to the short-λ enriched DLaN displayed a significantly increased number of cFos positive cells in both the pHb and BLA (Fig. 5A,B; Table 6) but not in hypothalamic regions of interest (S. Fig. 6; Table 6). In contrast, the long-λ enriched DLaN did not induce cFos expression in any of these regions (Fig. 5A,B; S. Fig. 6; Table 6). Prior work suggested that the glutamatergic cell population in the BLA is a critical part of a circuit responsible for repetitive behavior (Felix-Ortiz et al., 2016). Therefore, we crossed the *Cntnap2* KO line into mice expressing both vGAT2-Cre (Vong et al., 2011) and a Cre-dependent reporter ZsGreen1 (Ai6) (Madisen et al., 2010), which provide strong cell body labelling. WT and *Cntnap2* KO mice with these reporters were then exposed to short-λ enriched DLaN for two weeks. A robust expression of the vGlut2-ZsGreen1 reporter within the BLA region could be observed in both the WT and mutants (Fig. 5C). Most importantly, the short-λ DLaN elicited a higher number of vGlut2-ZsGreen1-cFos immunopositive in the *Cntnap2* KO mice (Fig. 5C,D; Table 7) in comparison to the WT under DLaN or the WT and mutants under LD conditions. Both genotypes exhibited a significantly higher co-expression in the light-treated group (Table 7). These data suggest that the glutamatergic cells within the BLA are activated by DLaN and raise the possibility that this cell population contributes to its effect on repetitive behavior.

4. Discussion

Nightly light exposure is a common environmental perturbation and has been shown to cause a number of ill effects (Lucassen et al., 2016; Bumgarner and Nelson, 2021).

Importantly, certain individuals may be more vulnerable to some undesirable effects of the exposure of light at night. For example, in the *Cntnap2* KO mouse model of ASD, we reported that DLaN selectively increases repetitive behavior, as measured by grooming, while WT mice were not impacted (Wang et al., 2020). On the other hand, DLaN negatively affected other behaviors including social interactions and daily activity rhythms in both *Cntnap2* KO and WT mice. In the present study, we confirmed these negative effects of nocturnal lighting on activity rhythms, social interactions, and repetitive behaviors (Table 3). Logically, the simplest approach to reducing these negative effects would solely be to decrease light intensity at night while ensuring a robust exposure to sunlight during the day. However, according to surveys, people spend a majority of time indoors (as high as 90%) and have need for illumination after the sun sets (e.g. Klepeis et al., 2001). Therefore, an appealing alternative approach would be to adjust the spectral quality of indoor lighting to minimize the undesirable effects. As a test case, in the present study, we used an array of LEDs to generate dim illumination (10 lx) to determine whether the spectral composition of nightly illumination would make a difference in WT and/or *Cntnap2* KO mice.

The retinal photoreceptor system has unique intensity and wave-length dependent characteristics (Lucas et al., 2014). The detrimental effects of nightly light exposure are likely to be mediated by ipRGCs expressing the photopigment melanopsin, which is maximally sensitive to light with a peak response to ≈480 nm light (Hattar et al., 2002; Panda et al., 2005). Indeed, a number of studies have found evidence that short-λ enriched lighting is more effective for circadian responses (for review see Brown, 2020). However, recent work emphasizes that ipRGCs also receive input from rod and cone photoreceptors (Hattar et al., 2002; Dacey et al., 2005; Güler et al., 2008; Lucas et al., 2012; Van Diepen et al., 2021; Schoonderwoerd et al., 2022) with rods driving the circadian response to low-intensity light (Altimus et al., 2010; Lall et al., 2010) like the 10 lx used in the present study. Here, we used an LED lighting system (Korrus Inc.) to tailor the spectral properties of the DLaN with the goal of manipulating melanopic stimulation. The output of the LEDs was measured as power over a defined wavelength (380–780 nm) using a spectrophotometer (S. Fig. 1). These data were analyzed using a CIE toolkit which enabled us to estimate that the short-λ illumination was at 15 melanopic lx and the long-λ illumination at 1 melanopic lx while maintaining illuminance at ≈10 lx. The M/P ratio (melanopic lx divided by photopic lx) was estimated to be at 1.49 and 0.11 for the short- and long-λ enriched lighting, respectively.

Using these two lighting treatments with predicted high and low melanopic stimulation, we measured the impact of the illumination on three classic tests of the ipRGC input to the circadian system (Fig. 1), showing that the low melanopic stimulation reduced the effect of light on negative masking, light-induced phase shifts and light-induction of cFos in the SCN. Next, we reported that the high melanopic illumination showed a greatly diminished ability to disrupt activity rhythms in *Opn4*^{DTA} mice, which lack ipRGCs (S. Fig. 2). Together, these data indicate that the ipRGCs are required for a majority of the negative effects of DLaN and that controlling melanopic stimulation altered activation of the ipRGC/SCN pathway. These findings, however, do not permit the identification of the photopigment responsible for the effects of DLaN as multiple photoreceptors convey information through the ipRGCs (see above).

With this validated lighting system in hand, we sought to use the LED array to determine whether long-λ enriched illumination would diminish DLaN disruption of behavior in WT and *Cntnap2* KO mice. Both lines of mice exhibited a significant reduction in a number of activity rhythm parameters when exposed to the high melanopic illumination, while the low melanopic illumination did not produce significant changes compared to LD control (Figs. 2, 3). Similarly, exposure to high melanopic illumination, but not to low melanopic DLaN, disrupted social interactions in both genotypes (Fig. 4). Finally, exposure to high melanopic illumination increased repetitive grooming in the *Cntnap2* KO, but not to the low melanopic DLaN (Fig. 4). Together, these data show that minimizing the melanopic activation of the light source was an effective strategy to minimize the undesirable effects of night-time light exposure.

In rodents, thresholds for negative masking are dependent on the wavelength (e.g. Walbeek et al., 2021). In the present study, we show some evidence that the long-λ illumination actually stimulated locomotor activity. First, in the masking experiments, 3 out of the 11 mice exposed to the long-λ illumination indeed showed increased activity (Fig. 1A). In addition, when examining the waveform of locomotor activity of the mice under long-λ illumination, the nocturnal activity was augmented in comparison to untreated controls (Fig. 2B) with many of the time points being significantly different. While we did not further explore this observation in the present study, there may well be conditions in which the long-λ illumination enhances activity levels and evokes other biological effects.

There is a strong male bias in ASD prevalence with a common reported ratio of ~4:1 (Fombonne, 2009) along with evidence for significant interactions between sex and genotype for the *Cntnap2* gene in human populations (e.g. Hsu et al., 2019). Some of these sex differences may be driven in part by male/female differences in phenotypic presentation, including fewer repetitive behaviors in females (e.g. Werling and Geschwind, 2013). On the other hand, sleep disturbances appear to be more common in female with ASD (Elkhatib Smidt et al., 2021). Prior work with the *Cntnap2* KO mouse model found clear evidence for sex difference in home cage activity with robust hypo-activity in the males but not in the females (Angelakos et al., 2019). In addition, the functional responses of cortical circuitry are more strongly affected by *Cntnap2* mutations in male than female mice (Townsend and Smith, 2017). Therefore, we powered the sample size to be able to examine possible sex differences. Sex differences could be observed in the activity rhythms in WT mice but were lost in the *Cntnap2* KO line (Table 4; S. Fig. 4). Interestingly, prior work has found that LPS-induced maternal immune activation caused male-specific deficits in behavior and gene expression in the *Cntnap2* KO line (Schaafsma et al., 2017). Thus, we asked whether the female mice might be less influenced by the environmental challenge caused by DLaN treatment. In the three behavioral assays (activity, grooming, and social interactions), we found that both sexes were negatively impacted by the DLaN (Table 5; S. Fig. 5). Overall, our data demonstrate that both sexes were negatively impacted by the *Cntnap2* mutation and the environmental disruption DLaN.

Prior work has shown that activation of ipRGC can drive cFos expression in several brain regions including those in the hypothalamus and limbic system (Milosavljevic et al., 2016; Fernandez et al., 2018). We sought to determine whether the 2-weeks of chronic DLaN

would alter cFos expression in some of those brain regions (Fig. 5A,B; S. Fig. 6). We did find that the high melanopic DLaN increased cFos expression in the pHb and BLA. Prior work has implicated the pHb as a region critically involved in the effects of light on mood (Fernandez et al., 2018). Specifically, there is support for circuit by which the ipRGC regulation of the dorsal region of the pHb projects to the nucleus accumbens (NAc) to drive depressive-like behaviors (An et al., 2020). Thus, we should expect to see DLaN driven alterations in depressive behavior in our mouse models (Fonken et al., 2012; Bedrosian et al., 2013; Walker 2nd et al., 2020) and this will be an important area for future work. More critical for the present study, prior work suggests that the BLA may regulate repetitive behavior (Felix-Ortiz and Tye, 2014; Sun et al., 2019). Using a reporter for the glutamate transporter vGlut2, we were able to show that cFos induction occurred robustly, although certainly not exclusively, in the glutamatergic cell population in the BLA (Fig. 5C,D). Therefore, we speculate that the DLaN driven activation of the glutamatergic cell population in the BLA contributes to the grooming behavior observed in the present study. However, we are also mindful that the cFos induction in the BLA occurred in both genotypes while only the mutant mice exhibited the increase in grooming so more experiments are required to evaluate this model.

This study was designed with possible translational implications in mind but does have a number of limitations. While mutations and polymorphisms in the *Cntnap2* gene are strongly associated with ASD (Peñagarikano and Geschwind, 2012), most diagnosis of ASD do not have a clear etiology, hence, finding in the *Cntnap2* mouse model may not prove to be generalizable. Still, while no animal model captures the full complexity of ASD, genetic models are extremely useful for studying the mechanism underlying specific symptoms (i.e. sleep and circadian disruption) (e.g. Möhrle et al., 2020). One particular concern in this study is that the mouse visual system has evolved to serve the distinct needs of nocturnal organisms and these are understandably distinct from diurnal primates. The melanopsin expressing retinal ganglion cell population exists in both nocturnal rodents and diurnal humans (e.g. Dacey et al., 2005) but the properties of this light detection system are different. Thus, the impact of changing the spectral composition of light will need to be explored in human subjects if we hope to extend these finding. Toward that end, we report our illumination parameters in energy units and in M/P ratios so that the illumination used in the present study can be compared to other lighting conditions. We should also be clear that we did not design this study to identify the photo-pigments that mediate the effects of dim light at night. The data do support a role for ipRGCs in mediating the effects of DLaN but, as described above, both rods and cones synapse onto the ipRGCs. Finally, while our work did identify a cell population in the BLA that could mediate the effects of DLaN on repetitive behaviors, future work will need to specifically test this hypothesis using optogenetic or chemogenetic approaches. Because of these limitations, more work is required, and caution should be used in the interpretation of our results.

With rapidly growing studies reporting the effects of lights on, not only circadian rhythms, but also general brain health (Stevenson et al., 2015; Lunn et al., 2017; Bumgarner and Nelson, 2021), the consequences of worldwide prevalence of DLaN should be seriously taken into concern for disease management, especially for patients with neurodevelopmental disorders and neurodegenerative diseases who are more vulnerable to environmental

perturbations. Many people spend the majority of time under artificial lighting, and their exposure to DLaN needs to be carefully considered. Inappropriate light at night is common in hospitals, long-term care centers, and even our homes (Fournier and Wirz-Justice, 2010; Burgess and Molina, 2014; Osibona et al., 2021; Xiao et al., 2021). Thus, nightly light pollution is a very common environmental disruption to our circadian rhythms all over the world, and the present study shows that the undesired outcomes of DLaN on sleep/wake cycles and autistic behavior can be lessened by tailoring the spectral content of light sources to minimize melanopic stimulation in a mouse model. Determining whether altering the spectral properties of light at night can also impact human health will be an important area for future work.

Supplementary Material

Refer to Web version on PubMed Central for supplementary material.

Acknowledgments

We would like to acknowledge UCLA students Kyle Nguyen-Ngo and Kelly Yun who helped with the scoring of some of the fluorescence staining. Dr. Kathy Tamai provided editorial assistance. We thank Dr. Stuart Peirson for advice on the illumination and providing software (Rodent Toolbox v2.2). Core equipment used in this study was supported by the National Institute of Child Health Development under award number: P50HD103557 (PIs Bookheimer, Kornblum). HBW was supported by a government scholarship for study abroad provided by the Taiwan Ministry of Education (#1100090595). An earlier version of this work was published as preprint, https://www.biorxiv.org/content/10.1101/2022.06.09.494760v2.

Data availability

Data will be made available on request.

Abbreviations:

ANOVA	analysis of variance
ASD	autism spectrum disorders
DD	constant darkness
***Cntnap2* KO**	contactin-associated protein-like 2 knock out
DLaN	dim light at night
ipRGCs	intrinsically photosensitive retinal ganglion cells
LD	light:dark
LED	light-emitting diode
SEM	standard error of the mean
SCN	suprachiasmatic nucleus
λ	wavelength

WT	wild-type
ZT	Zeitgeber Time

References

Altimus CM, Güler AD, Alam NM, Arman AC, Prusky GT, Sampath AP, Hattar S, 2010. Rod photoreceptors drive circadian photoentrainment across a wide range of light intensities. Nat. Neurosci 13 (9), 1107. [PubMed: 20711184]

An K, Zhao H, Miao Y, Xu Q, Li Y-F, Ma Y-Q, Shi Y-M, Shen J-W, Meng J-J, Yao Y-G, 2020. A circadian rhythm-gated subcortical pathway for nighttime-light-induced depressive-like behaviors in mice. Nat. Neurosci 23 (7), 869–880. [PubMed: 32483349]

Angelakos CC, Tudor JC, Ferri SL, Jongens TA, Abel T, 2019. Home-cage hypoactivity in mouse genetic models of autism spectrum disorder. Neurobiol. Learn. Mem 165, 107000 10.1016/j.nlm.2019.02.010. [PubMed: 30797034]

Baker EK, Richdale AL, 2017. Examining the behavioural sleep-wake rhythm in adults with autism spectrum disorder and no comorbid intellectual disability. J. Autism Dev. Disord 47 (4), 1207–1222. [PubMed: 28160224]

Bedrosian TA, Fonken LK, Walton JC, Nelson RJ, 2011. Chronic exposure to dim light at night suppresses immune responses in Siberian hamsters. Biol. Lett 7 (3), 468–471. 10.1098/rsbl.2010.1108. [PubMed: 21270021]

Bedrosian TA, Vaughn CA, Galan A, Daye G, Weil ZM, Nelson RJ, 2013. Nocturnal light exposure impairs affective responses in a wavelength-dependent manner. J. Neurosci 33 (32), 13081–13087. [PubMed: 23926261]

Brown TM, 2020. Melanopic illuminance defines the magnitude of human circadian light responses under a wide range of conditions. J. Pineal Res 69 (1), e12655 10.1111/jpi.12655. [PubMed: 32248548]

Bumgarner JR, Nelson RJ, 2021. Light at night and disrupted circadian rhythms alter physiology and behavior. Integr. Comp. Biol 61 (3), 1160–1169. 10.1093/icb/icab017. [PubMed: 33787878]

Burgess HJ, Molina TA, 2014. Home lighting before usual bedtime impacts circadian timing: a field study. Photochem. Photobiol 90 (3), 723–726. [PubMed: 24918238]

Chew KS, Renna JM, McNeill DS, Fernandez DC, Keenan WT, Thomsen MB, Ecker JL, Loevinsohn GS, VanDunk C, Vicarel DC, Tufford A, Weng S, Gray PA, Cayouette M, Herzog ED, Zhao H, Berson DM, Hattar S, 2017. A subset of ipRGCs regulates both maturation of the circadian clock and segregation of retinogeniculate projections in mice. Elife 6, e22861 10.7554/eLife.22861. [PubMed: 28617242]

Cohen S, Conduit R, Lockley SW, Rajaratnam SMW, Cornish KM, 2014. The relationship between sleep and behavior in autism spectrum disorder (ASD): a review. J. Neurodev. Disord 6 (1), 44. 10.1186/1866-1955-6-44. [PubMed: 25530819]

Dacey DM, Liao HW, Peterson BB, Robinson FR, Smith VC, Pokorny J, Yau KW, Gamlin PD, 2005. Melanopsin-expressing ganglion cells in primate retina signal colour and irradiance and project to the LGN. Nature 433 (7027), 749–754. 10.1038/nature03387 [PubMed: 15716953]

Devnani P, Hegde A, 2015. Autism and sleep disorders. J. Pediatr. Neurosci 10 (4), 304–307. 10.4103/1817-1745.174438. [PubMed: 26962332]

Dong H-Y, Wang B, Li H-H, Yue X-J, Jia F-Y, 2021. Correlation between screen time and autistic symptoms as well as development quotients in children with autism spectrum disorder. Front. Psychiatry 12, 140.

Elkhatib Smidt SD, Hitt T, Zemel BS, Mitchell JA, 2021. Sex differences in childhood sleep and health implications. Ann. Hum. Biol 48 (6), 474–484. 10.1080/03014460.2021.1998624. [PubMed: 35105205]

Engelhardt CR, Mazurek MO, Sohl K, 2013. Media use and sleep among boys with autism spectrum disorder, ADHD, or typical development. Pediatrics 132 (6), 1081–1089. Epub 2013/11/20. 10.1542/peds.2013-2066. [PubMed: 24249825]

Felix-Ortiz AC, Burgos-Robles A, Bhagat ND, Leppla CA, Tye KM, 2016. Bidirectional modulation of anxiety-related and social behaviors by amygdala projections to the medial prefrontal cortex. Neuroscience 321, 197–209. 10.1016/j.neuroscience.2015.07.041. [PubMed: 26204817]

Felix-Ortiz AC, Tye KM, 2014. Amygdala inputs to the ventral hippocampus bidirectionally modulate social behavior. The Journal of Neuroscience 34, 586–595. 10.1523/JNEUROSCI.4257-13.2014. [PubMed: 24403157]

Fernandez DC, Fogerson PM, Lazzerini Ospri L, Thomsen MB, Layne RM, Severin D, Zhan J, Singer JH, Kirkwood A, Zhao H, Berson DM, Hattar S, 2018. Light affects mood and learning through distinct retina-brain pathways. Cell 175 (1), 71–84.e18. 10.1016/j.cell.2018.08.004. [PubMed: 30173913]

Figueiro MG, Pedler D, 2020. Red light: a novel, non-pharmacological intervention to promote alertness in shift workers. J. Saf. Res 74, 169–177.

Fonken LK, Kitsmiller E, Smale L, Nelson RJ, 2012. Dim nighttime light impairs cognition and provokes depressive-like responses in a diurnal rodent. J. Biol. Rhythm 27 (4), 319–327.

Fombonne E, 2009. Epidemiology of pervasive developmental disorders. Pediatr Res 65, 591–598. 10.1203/PDR.0b013e31819e7203. [PubMed: 19218885]

Fonken LK, Aubrecht TG, Meléndez-Fernández OH, Weil ZM, Nelson RJ, 2013a. Dim light at night disrupts molecular circadian rhythms and increases body weight. J. Biol. Rhythm 28 (4), 262–271. 10.1177/0748730413493862 .

Fonken LK, Weil ZM, Nelson RJ, 2013b. Mice exposed to dim light at night exaggerate inflammatory responses to lipopolysaccharide. Brain Behav. Immun 34, 159–163. 10.1016/j.bbi.2013.08.011. [PubMed: 24012645]

Foster RG, Hughes S, Peirson SN, 2020. Circadian Photoentrainment in Mice and Humans. Biology (Basel) 9 (7), 180. 10.3390/biology9070180. [PubMed: 32708259]

Fournier C, Wirz-Justice A, 2010. Light, health and wellbeing: implications from chronobiology for architectural design. World Health Design: Architecture, Culture, Technology 3 (3), 44–49.

Gladanac B, Jonkman J, Shapiro CM, Brown TJ, Ralph MR, Casper RF, Rahman SA, 2019. Removing short wavelengths from polychromatic white light attenuates circadian phase resetting in rats. Front. Neurosci 13, 954. 10.3389/fnins.2019.00954. [PubMed: 31551702]

Güler AD, Ecker JL, Lall GS, Haq S, Altimus CM, Liao HW, Barnard AR, Cahill H, Badea TC, Zhao H, Hankins MW, Berson DM, Lucas RJ, Yau KW, Hattar S, 2008. Melanopsin cells are the principal conduits for rod-cone input to non-image-forming vision. Nature 453 (7191), 102–105. 10.1038/nature06829. [PubMed: 18432195]

Hattar S, Liao HW, Takao M, Berson DM, Yau KW, 2002. Melanopsin-containing retinal ganglion cells: architecture, projections, and intrinsic photosensitivity. Science 295 (5557), 1065–1070. 10.1126/science.1069609. [PubMed: 11834834]

Healy S, Garcia JM, Haegele JA, 2020. Environmental factors associated with physical activity and screen time among children with and without autism spectrum disorder. J. Autism Dev. Disord 50 (5), 1572–1579. [PubMed: 30446873]

Hsu M, Dedhia M, Crusio WE, Delprato A, 2019. Sex differences in gene expression patterns associated with the APOE4 allele. F1000Res 8, 387. 10.12688/f1000research.18671.2 . [PubMed: 31448102]

Klepeis NE, Nelson WC, Ott WR, Robinson JP, Tsang AM, Switzer P, Behar JV, Hern SC, Engelmann WH, 2001 May-Jun. The National Human Activity Pattern Survey (NHAPS): a resource for assessing exposure to environmental pollutants. J. Expo. Anal. Environ. Epidemiol 11 (3), 231–252. 10.1038/sj.jea.7500165. [PubMed: 11477521]

Lall GS, Revell VL, Momiji H, Al Enezi J, Altimus CM, Güler AD, Aguilar C, Cameron MA, Allender S, Hankins MW, Lucas RJ, 2010. Distinct contributions of rod, cone, and melanopsin photoreceptors to encoding irradiance. Neuron 66 (3), 417–428. 10.1016/j.neuron.2010.04.037. [PubMed: 20471354]

Lazzerini Ospri L, Prusky G, Hattar S, 2017. Mood, the circadian system, and melanopsin retinal ganglion cells. Annu. Rev. Neurosci 40, 539–556. 10.1146/annurev-neuro-072116-031324. Jul 25. [PubMed: 28525301]

Lee FY, Wang H-B, Hitchcock O, Loh DH-W, Whittaker DS, Kim Y-S, Aiken A, Kokikian C, Dell'Angelica EC, Colwell CS, 2018. Sleep/wake disruption in a mouse model of BLOC-1 deficiency. Front. Neurosci 12, 759. [PubMed: 30498428]

Lucas RJ, Lall GS, Allen AE, Brown TM, 2012. Chapter 1 - how rod, cone, and melanopsin photoreceptors come together to enlighten the mammalian circadian clock. In: Andries Kalsbeek MMTR, Russell GF (Eds.), Prog Brain Res Elsevier, pp. 1–18.

Lucas RJ, Peirson SN, Berson DM, Brown TM, Cooper HM, Czeisler CA, Figueiro MG, Gamlin PD, Lockley SW, O'Hagan JB, 2014. Measuring and using light in the melanopsin age. Trends Neurosci 37 (1), 1–9. [PubMed: 24287308]

Lucassen EA, Coomans CP, van Putten M, de Kreij SR, van Genugten JH, Sutorius RP, de Rooij KE, van der Velde M, Verhoeve SL, Smit JW, Löwik CW, Smits HH, Guigas B, Aartsma-Rus AM, Meijer JH, 2016. Environmental 24-hr cycles are essential for health. Curr. Biol 26 (14), 1843–1853. 10.1016/j.cub.2016.05.038. [PubMed: 27426518]

Lunn RM, Blask DE, Coogan AN, Figueiro MG, Gorman MR, Hall JE, Hansen J, Nelson RJ, Panda S, Smolensky MH, Stevens RG, Turek FW, Vermeulen R, Carreón T, Caruso CC, Lawson CC, Thayer KA, Twery MJ, Ewens AD, Garner SC, Schwingl PJ, Boyd WA, 2017. Health consequences of electric lighting practices in the modern world: a report on the National Toxicology Program's workshop on shift work at night, artificial light at night, and circadian disruption. Sci. Total Environ 607–608, 1073–1084. 10.1016/jscitotenv.2017.07.056.

Madisen L, Zwingman TA, Sunkin SM, Oh SW, Zariwala HA, Gu H, Ng LL, Palmiter RD, Hawrylycz MJ, Jones AR, Lein ES, Zeng H, 2010. A robust and high-throughput Cre reporting and characterization system for the whole mouse brain. Nat. Neurosci 13 (1), 133–140. 10.1038/nn.2467. [PubMed: 20023653]

Matynia A, Parikh S, Chen B, Kim P, McNeill DS, Nusinowitz S, Evans C, Gorin MB, 2012. Intrinsically photosensitive retinal ganglion cells are the primary but not exclusive circuit for light aversion. Exp. Eye Res 105, 60–69. 10.1016/j.exer.2012.09.012. [PubMed: 23078956]

Mazurek MO, Sohl K, 2016. Sleep and behavioral problems in children with autism spectrum disorder. J. Autism Dev. Disord 46 (6), 1906–1915. 10.1007/s10803-016-2723-7. [PubMed: 26823076]

Mazurek MO, Engelhardt Cr Fau-Hilgard J, Hilgard J Fau-Sohl K, Sohl K, 2016. Bedtime electronic media use and sleep in children with autism spectrum disorder. J. Dev. Behav. Pediatr 37 (7), 525–531. 10.1097/DBP.0000000000000314 . [PubMed: 27355885]

Milosavljevic N, Cehajic-Kapetanovic J, Procyk CA, Lucas RJ, 2016. Chemogenetic activation of melanopsin retinal ganglion cells induces signatures of arousal and/or anxiety in mice. Curr. Biol 26 (17), 2358–2363. [PubMed: 27426512]

Möhrle D, Fernández M, Peñagarikano O, Frick A, Allman B, Schmid S, 2020. What we can learn from a genetic rodent model about autism. Neurosci. Biobehav. Rev 109, 29–53. 10.1016/j.neubiorev.2019.12.015. [PubMed: 31887338]

Mouland JW, Martial FP, Lucas RJ, Brown TM, 2021. Modulations in irradiance directed at melanopsin, but not cone photoreceptors, reliably alter electrophysiological activity in the suprachiasmatic nucleus and circadian behaviour in mice. J. Pineal Res 70 (4), e12735 10.1111/jpi.12735. [PubMed: 33793975]

Nagare R, Rea MS, Plitnick B, Figueiro MG, 2019a. Effect of white light devoid of "cyan" spectrum radiation on nighttime melatonin suppression over a 1-h exposure duration. J. Biol. Rhythm 34 (2), 195–204. 10.1177/0748730419830013.

Nagare R, Rea MS, Plitnick B, Figueiro MG, 2019b. Nocturnal melatonin suppression by adolescents and adults for different levels, spectra, and durations of light exposure. J. Biol. Rhythm 34 (2), 178–194. 10.1177/0748730419828056.

Osibona O, Solomon BD, Fecht D, 2021. Lighting in the home and health: a systematic review. Int. J. Environ. Res. Public Health 18 (2), 609. 10.3390/ijerph18020609. [PubMed: 33445763]

Panda S, Nayak SK, Campo B, Walker JR, Hogenesch JB, Jegla T, 2005. Illumination of the melanopsin signaling pathway. Science 307 (5709), 600–604. 10.1126/science.1105121. [PubMed: 15681390]

Peñagarikano O, Geschwind DH, 2012. What does CNTNAP2 reveal about autism spectrum disorder? Trends Mol. Med 18 (3), 156–163. 10.1016/j.molmed.2012.01.003. [PubMed: 22365836]

Plano SA, Casiraghi LP, García Moro P, Paladino N, Golombek DA, Chiesa JJ, 2017. Circadian and metabolic effects of light: implications in weight homeostasis and health. Front. Neurol 8, 558. 10.3389/fneur.2017.00558. [PubMed: 29097992]

Schaafsma SM, Gagnidze K, Reyes A, Norstedt N, Månsson K, Francis K, Pfaff DW, 2017. Sex-specific gene-environment interactions underlying ASD-like behaviors. Proc. Natl. Acad. Sci. U. S. A 114 (6), 1383–1388. 10.1073/pnas.1619312114. [PubMed: 28115688]

Schoonderwoerd RA, de Rover M, Janse JAM, Hirschler L, Willemse CR, Scholten L, Klop I, van Berloo S, van Osch MJP, Swaab DF, Meijer JH, 2022. The photobiology of the human circadian clock. Proc. Natl. Acad. Sci. U. S. A 119 (13), e2118803119. [PubMed: 35312355]

Shelton AR, Malow B, 2021. Neurodevelopmental disorders commonly presenting with sleep disturbances. Neurotherapeutics 18 (1), 156–169. 10.1007/s13311-020-00982-8. [PubMed: 33403472]

Stevenson TJ, Visser ME, Arnold W, Barrett P, Biello S, Dawson A, Denlinger DL, Dominoni D, Ebling FJ, Elton S, Evans N, Ferguson HM, Foster RG, Hau M, Haydon DT, Hazlerigg DG, Heideman P, Hopcraft JG, Jonsson NN, Kronfeld-Schor N, Kumar V, Lincoln GA, MacLeod R, Martin SA, Martinez-Bakker M, Nelson RJ, Reed T, Robinson JE, Rock D, Schwartz WJ, Steffan-Dewenter I, Tauber E, Thackeray SJ, Umstatter C, Yoshimura T, Helm B, 2015. Disrupted seasonal biology impacts health, food security and ecosystems. Proc. Biol. Sci 282 (1817), 20151453. 10.1098/rspb.2015.1453. [PubMed: 26468242]

Stiller A, Weber J, Strube F, Mößle T, 2019. Caregiver reports of screen time use of children with autism spectrum disorder: a qualitative study. Behav. Sci. (Basel) 9 (5), 56. 10.3390/bs9050056. [PubMed: 31121966]

Sun T, Song Z, Tian Y, Tian W, Zhu C, Ji G, Luo Y, Chen S, Wang L, Mao Y, 2019. Basolateral amygdala input to the medial prefrontal cortex controls obsessive-compulsive disorder-like checking behavior. Proc. Natl. Acad. Sci 116 (9), 3799–3804. [PubMed: 30808765]

Townsend LB, Smith SL, 2017. Genotype- and sex-dependent effects of altered Cntnap2 expression on the function of visual cortical areas. J. Neurodev. Disord 9, 2. 10.1186/s11689-016-9182-5. [PubMed: 28115996]

van Diepen HC, Schoonderwoerd RA, Ramkisoensing A, Janse JAM, Hattar S, Meijer JH, 2021. Distinct contribution of cone photoreceptor subtypes to the mammalian biological clock. Proc. Natl. Acad. Sci. U. S. A 118 (22), e2024500118 10.1073/pnas.2024500118. [PubMed: 34050024]

Vethe D, Scott J, Engstrøm M, Salvesen Ø, Sand T, Olsen A, Morken G, Heglum HS, Kjørstad K, Faaland PM, 2021. The evening light environment in hospitals can be designed to produce less disruptive effects on the circadian system and improve sleep. Sleep 44 (3), 194.

Vong L, Ye C, Yang Z, Choi B, Chua S Jr., Lowell BB, 2011. Leptin action on GABAergic neurons prevents obesity and reduces inhibitory tone to POMC neurons. Neuron 71 (1), 142–154. 10.1016/j.neuron.2011.05.028. [PubMed: 21745644]

Walbeek TJ, Harrison EM, Gorman MR, Glickman GL, 2021. Naturalistic intensities of light at night: a review of the potent effects of very dim light on circadian responses and considerations for translational research. Front. Neurol 12, 625334 10.3389/fneur.2021.625334. [PubMed: 33597916]

Walker WH 2nd, Borniger JC, Gaudier-Diaz MM, Hecmarie Meléndez-Fernández O, Pascoe JL, Courtney DeVries A, Nelson RJ, 2020. Acute exposure to low-level light at night is sufficient to induce neurological changes and depressive-like behavior. Mol. Psychiatry 25 (5), 1080–1093. 10.1038/s41380-019-0430-4. [PubMed: 31138889]

Wang H-B, Whittaker DS, Truong D, Mulji AK, Ghiani CA, Loh DH, Colwell CS, 2017. Blue light therapy improves circadian dysfunction as well as motor symptoms in two mouse models of Huntington's disease. Neurobiol. Sleep Circadian Rhythm 2, 39–52. 10.1016/j.nbscr.2016.12.002.

Wang H-B, Loh DH, Whittaker DS, Cutler T, Howland D, Colwell CS, 2018. Time-restricted feeding improves circadian dysfunction as well as motor symptoms in the Q175 mouse model of Huntington's disease. eNeuro 5 (1) 10.1523/ENEURO.0431-17.2017.ENEURO.0431-17.2017.

Wang HB, Tahara Y, Luk SHC, Kim Y-S, Hitchcock ON, Kaswan ZAM, Kim YI, Block GD, Ghiani CA, Loh DH, 2020. Melatonin treatment of repetitive behavioral deficits in the Cntnap2 mouse model of autism spectrum disorder. Neurobiol. Dis 145, 105064. [PubMed: 32889171]

Werling DM, Geschwind DH, 2013. Sex differences in autism spectrum disorders. Curr. Opin. Neurol 26 (2), 146–153. 10.1097/WCO.0b013e32835ee548. [PubMed: 23406909]

Xiao H, Cai H, Li X, 2021. Non-visual effects of indoor light environment on humans: a review. Physiol. Behav 228 10.1016/j.physbeh.2020.113195, 113195. Jan 1. [PubMed: 33022281]

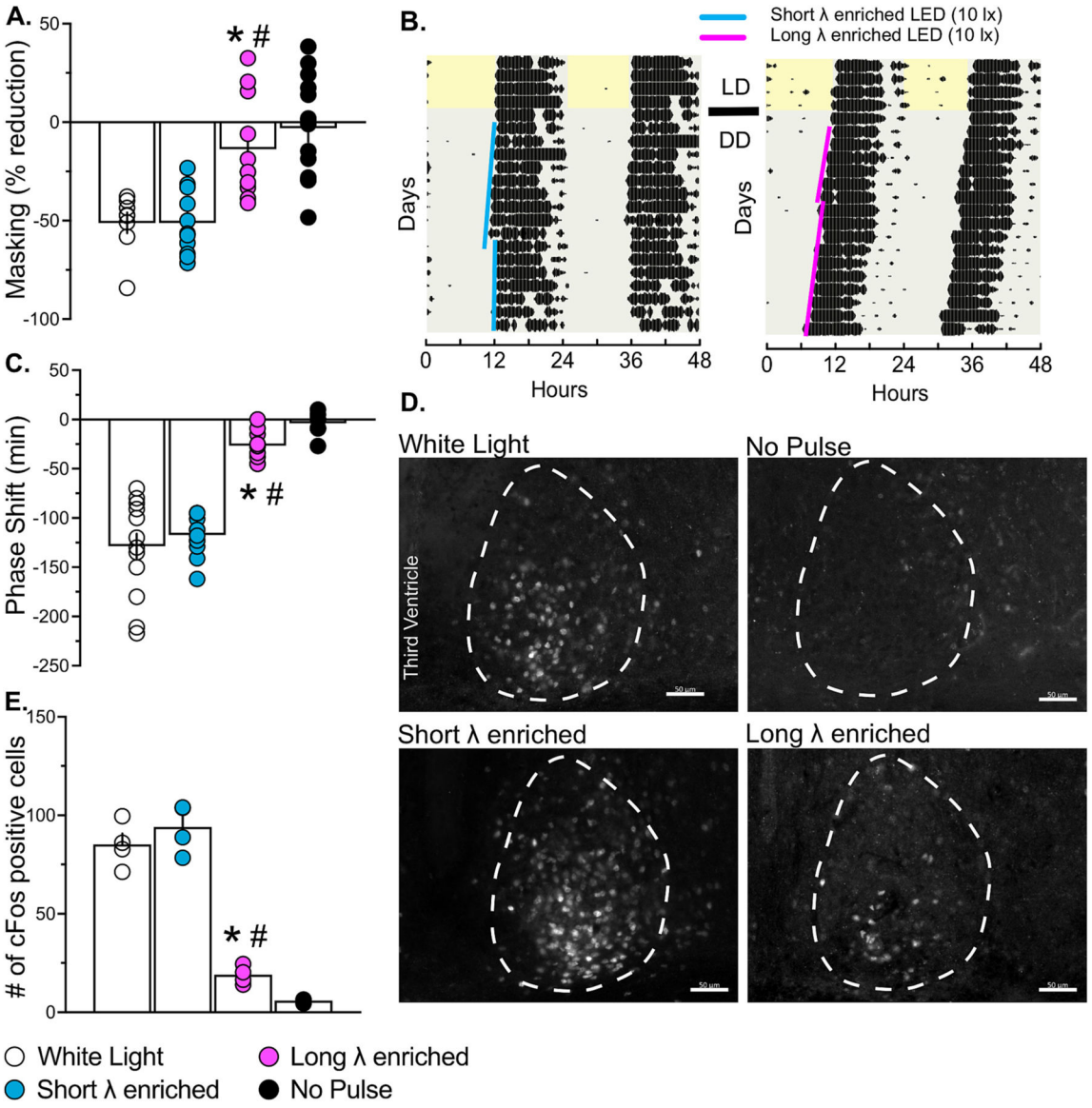

Fig. 1.

Shift to longer wavelength illumination reduces negative masking, light-induced phase shifts of the circadian activity rhythms, and induction of cFos in the suprachiasmatic nucleus of WT mice. (A) The long-λ enriched light elicited a much lower suppression of activity. Light-induced masking of activity in WT mice held in a light:dark (LD) cycle and exposed to white light (50 lx), the short- or long-λ enriched light (10 lx) for one hour at ZT 14. The activity level during this light exposure was compared to that during the equivalent time (ZT 14–15) on the day before the treatment (baseline activity). (B,C) Lower effects of the long-λ enriched light on light-induced phase shifts. (B) Examples of light-induced phase shifts of wheel-running activity onsets. After entrainment to the LD cycle, WT mice were placed into constant darkness (DD) for 10 days and then exposed to white light (10 lx for 1, not shown), the short- or long-λ enriched illumination (10 lx for 15 min) at CT 16 (4 h after the activity onset). The blue or magenta solid lines show the activity onset

before and after light treatment with the short- or long-λ enriched illumination, respectively. (C) The short-λ enhanced illumination produced a significant phase delay of the circadian system. (D,E) The short-λ, but not the long-λ, enhanced illumination produced a significant increase in the number of cFos positive cells in the SCN. (D) Examples of light-evoked cFos expression in the suprachiasmatic nucleus (SCN). The boundaries of the SCN are shown by the dashed line. Mice were held in DD for 10 days and then exposed to white light (10 lx), the short- or long-λ enriched illumination (10 lx) for 15 min at CT 16, perfused 45 min later and the brains collected. (E) Cells were counted in both the left and right SCN in two consecutive coronal sections per animal and the numbers averaged to obtain one value per animal. The histograms show the means ± the standard error of the mean (SEM) with the values from the individual animals overlaid. Data were analyzed using one-way ANOVA (Table 1) followed by the Holm-Sidak multiple comparisons' test with the asterisks indicating significant difference vs the white light and the crosshatch vs the short-λ enhanced illumination ($P < 0.05$). (For interpretation of the references to colour in this figure legend, the reader is referred to the web version of this article.)

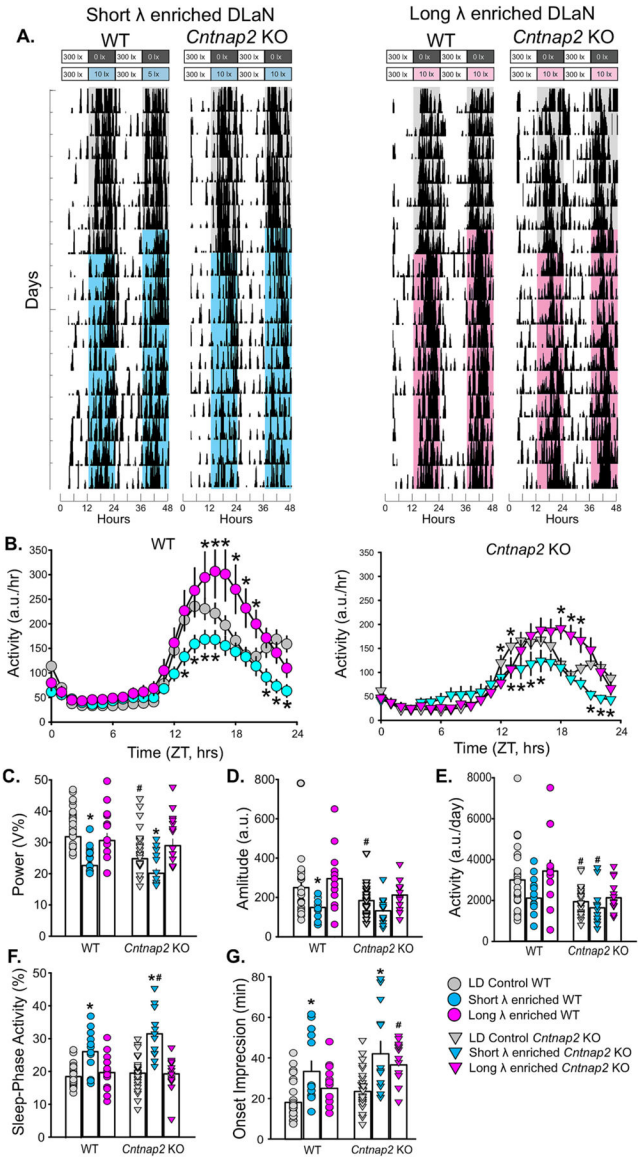

Fig. 2.

Long wavelength illumination minimizes DLaN disruption of daily activity rhythms in WT and *Cntnap2* KO mice. (A) Examples of actograms of daily rhythms in cage activity of WT and *Cntnap2* KO mice exposed to a short-λ (left) or a long-λ (right) enriched DLaN (10 lx) for 2 weeks. The activity levels in the actograms were normalized to the same scale (85% of the maximum of the most active individual. Each row represents two con*sec*utive days, and the second day is repeated at the beginning of the next row. The bars on the top of actograms indicates the time and intensity when the nightly lights were given. The cyan shading represents the short-λ enhanced lighting and the magenta shading the long-λ enhanced lighting. (B) Waveforms of daily rhythms in cage activity under short-λ (teal) or long-λ (magenta) enriched DLaN in WT (circles) and *Cntnap2* KO (triangles) mice. Values from mice in control conditions (LD) are shown for comparison (grey). The activity waveform (1 h bins) of each group was analyzed using a two-way ANOVA for repeated

measures with treatment and time as factors. Both groups exhibited significant effects of time (WT: $F_{(23,1151)} = 43.29$, $P < 0.001$; *Cntnap2* KO: $F_{(23,1151)} = 44.96$, $P < 0.001$) and treatment (WT: $F_{(2,1151)} = 42.66$, $P < 0.001$; *Cntnap2* KO: $F_{(2,1151)} = 15.16$, $P < 0.001$), and a significant interaction between the two factors was identified (WT: $F_{(46,1151)} = 2.57$, $P < 0.001$; *Cntnap2* KO: $F_{(46,1151)} = 3.8$, $P < 0.001$). Asterisks indicate significant ($P < 0.05$) differences between the 1 h bins as measured by Holm-Sidak test for multiple comparisons. (C-G) Properties of the daily activity rhythms (10-days recordings) in control LD condition and exposed to short or long λ enhanced DLaN were analyzed using a two-way ANOVA with genotype and treatment as factors followed by the Holm-Sidak test for multiple comparisons ($n = 12$ per genotype/treatment group; see also Table 3). Histograms show the means ± SEM with the values from the individual animals overlaid. Significant ($P < 0.05$) differences as a result of the treatment within or between genotypes are indicated with an asterisk or a crosshatch, respectively. a.u. = arbitrary units. (For interpretation of the references to colour in this figure legend, the reader is referred to the web version of this article.)

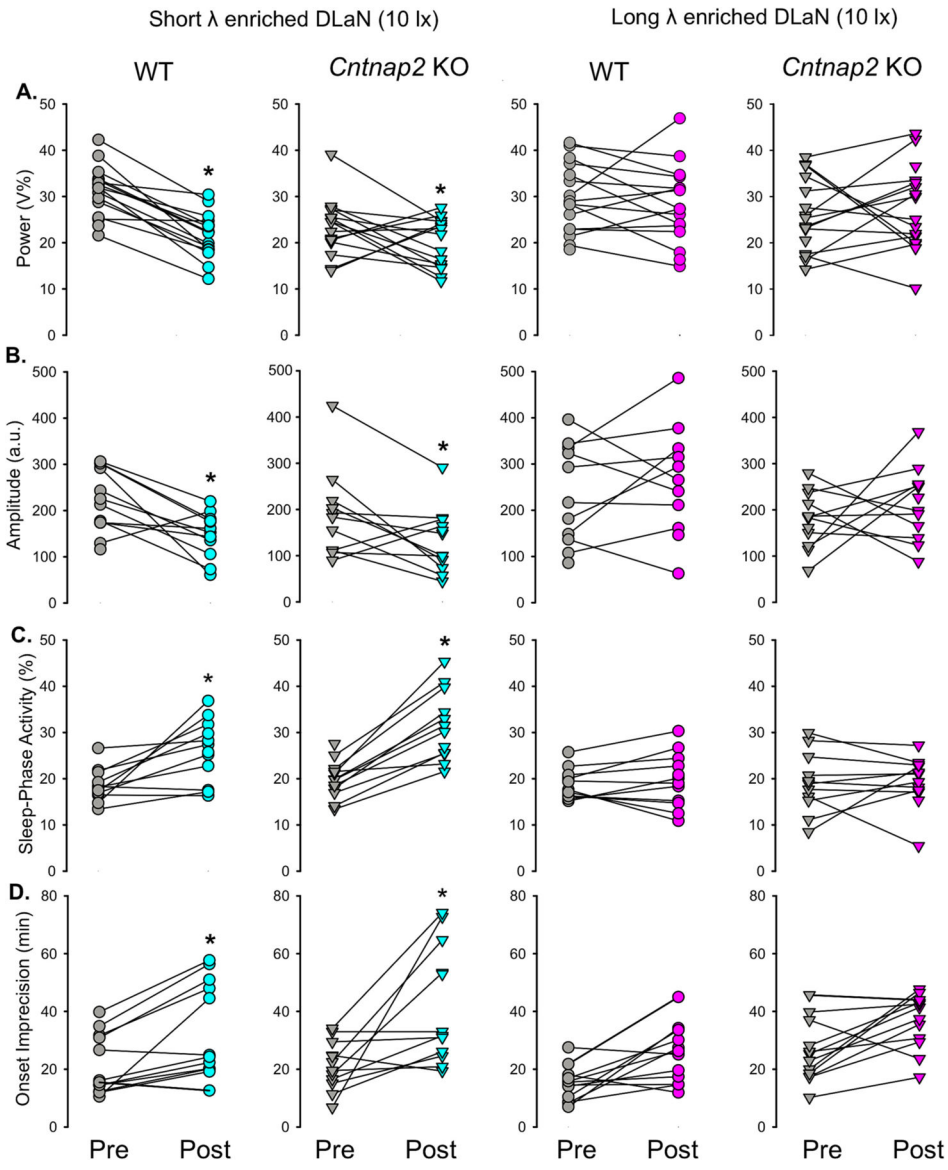

Fig. 3.

Long wavelength illumination was less disruptive to the activity rhythms of WT and *Cntnap2* KO mice. Key parameters of the daily activity rhythms before (grey) and after exposure to the short-λ (teal) or the long-λ (magenta) enriched DLaN treatment were analyzed in each individual mouse to better visualize the animal-to-animal variability in the response to the illumination. Values from individual WT (circles) and *Cntnap2* KO (triangles) mice are reported and an asterisk over the treated values indicates significant difference ($P < 0.05$, Paired *t*-test). The paired t-test provides a sensitive tool to determine if the DLaN treatment caused a change in comparison to pre-treatment values without a comparison between the genotypes. (For interpretation of the references to colour in this figure legend, the reader is referred to the web version of this article.)

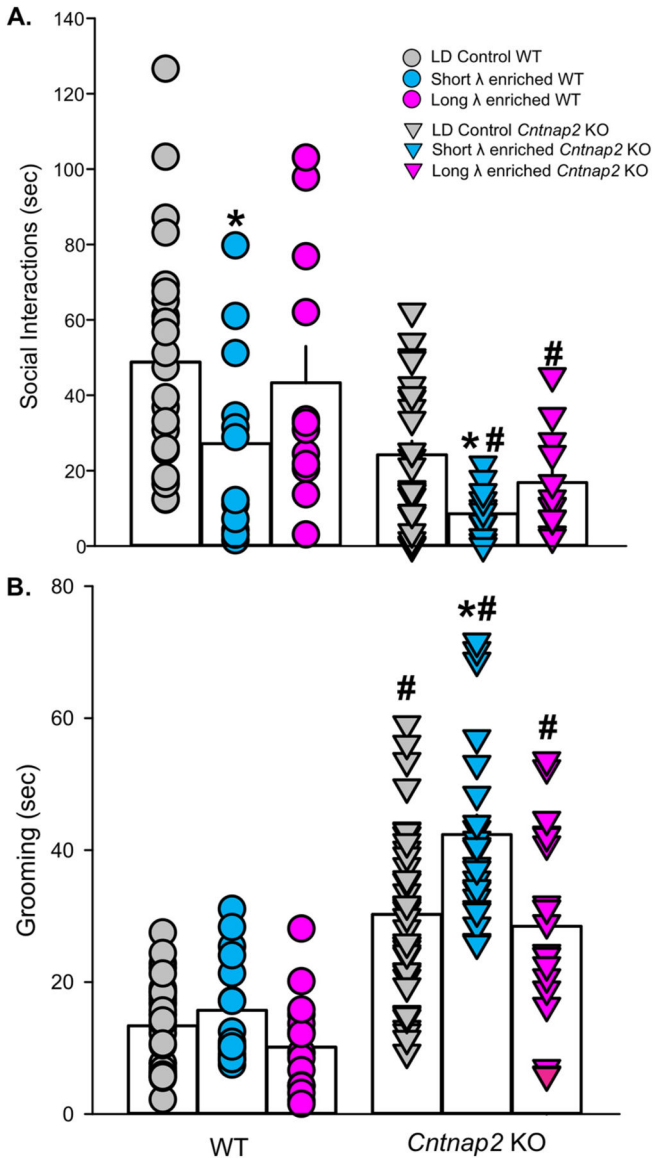

Fig. 4.

Long wavelength illumination lessened DLaN-evoked social deficits in WT and *Cntnap2* KO mice as well as repetitive behavior in the *Cntnap2* KO mice. (A) Time spent in social interactions is significantly reduced in WT and mutants exposed to the short-λ enriched DLaN. Social behavior was evaluated by analyzing the time actively spent by the testing mouse in interactions with the novel stranger mouse. The stranger and testing mice were matched for age, sex and genotype. Experiments were conducted during the active phase at ZT 18. (B) The mutants displayed increased grooming behavior in all the lighting conditions in comparison to the WT, but exposure to the short-λ enriched DLaN further affected this measure of repetitive behavior. Grooming was assessed in a novel arena under each of the three lighting condition (LD, short-λ or long-λ enriched DLaN). Tests were conducted at ZT 18. Histograms show the means ± SEM with overlaid the values from individual WT (circles) and *Cntnap2* KO (triangles) mice in LD (grey) and under the

short-λ (teal) or the long-λ (magenta) enriched DLaN. Data were analyzed using a two-way ANOVA with genotype and treatment as variable (see Table 3) followed by the Holm-Sidak multiple comparisons' test. The asterisks indicate significant differences ($P < 0.05$) between LD and DLaN treatments within genotype and the crosshatches between genotypes. (For interpretation of the references to colour in this figure legend, the reader is referred to the web version of this article.)

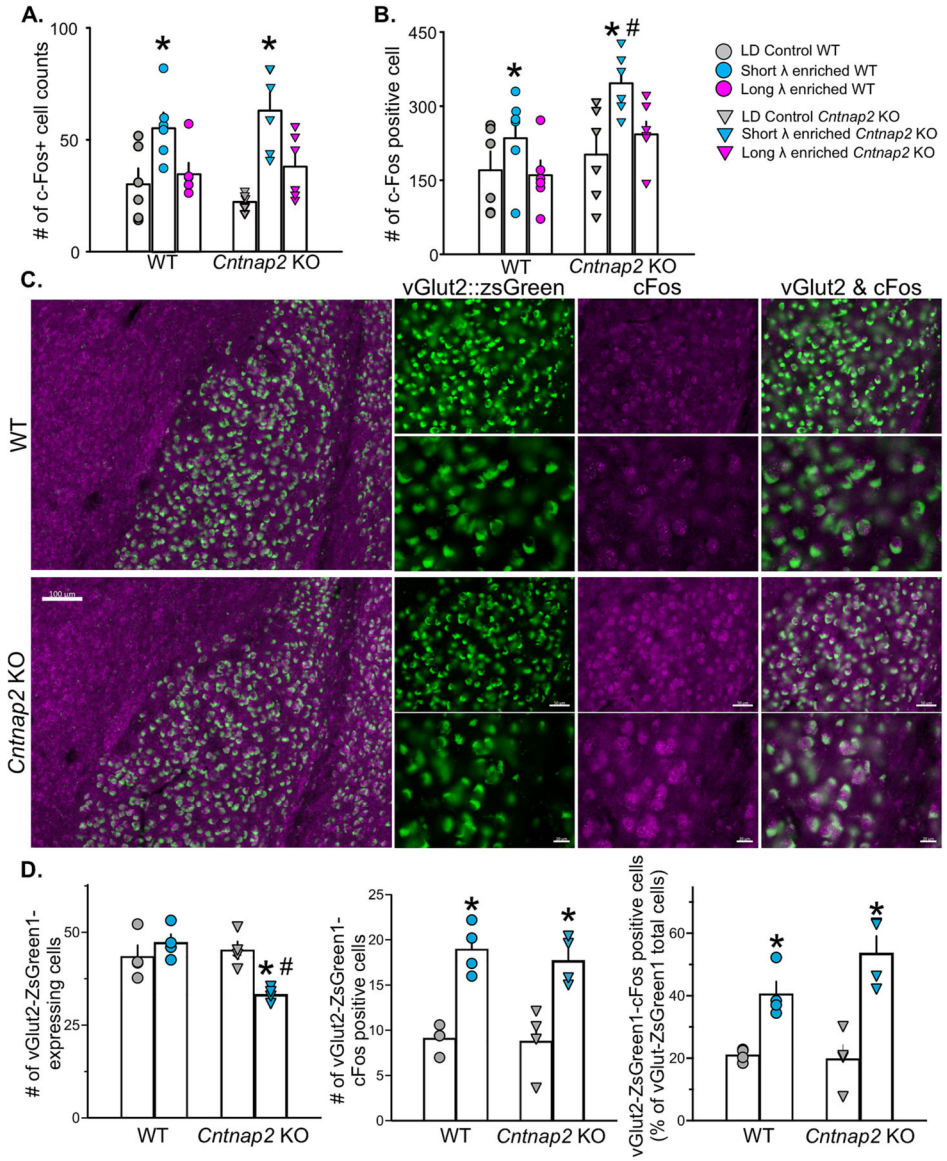

Fig. 5.

The short, but not the long, wavelength illumination elicits a selective increase in cFos immunopositive cells in the peri-habenula and the basolateral amygdala. Brains were collected at ZT 18 from WT (circles) and *Cntnap2* KO (triangles) mice held in LD, or exposed to the short-λ (teal) or long-λ (magenta) enriched DLaN (10 lx) for two weeks. Quantification of the cFos positive cells in the peri-habenular region (A) and the basolateral amygdala (BLA) (B). The number of cFos positive cells was determined bilaterally in both regions. The values from two con*sec*utive slices/animal (both left and right hemisphere) were averaged to obtain one value per animal ($n = 6$), and are shown as the mean ± SEM (histograms with the values from the individual animals overlaid). Data were analyzed with a two-way ANOVA with genotype and treatment as factors (see Table 6) followed by Holm-Sidak multiple comparisons' test. Significant ($P < 0.05$) effects of treatment within or between genotypes are indicated with an asterisk or a crosshatch, respectively.

(C) Representative images of vGlut2-ZsGreen1 neurons immunopositive for cFos in the BLA of WT and *Cntnap2* KO mice. WT and *Cntnap2* KO mice heterozygous for vGlut2-ZsGreen1 were held in LD or exposed to the short-λ enriched DLaN for two weeks. Mice were then perfused at ZT18, the brains collected and immunostained for cFos. (D) The *Cntnap2* KO mice exposed to the short-λ enriched DLaN display a lower number of vGlut2-ZsGreen1 cells. This lighting condition elicited a significant increase in the number of cFOS positive cells in both genotypes. But exposure to the short-λ enriched DLaN activated more glutamatergic neurons in the mutants in comparison to the WT. cFosThe total number of vGlut2-ZsGreen1 neurons and, among these, of those immunopositive for cFos was determined in 4 to 7 images acquired at random from 6 consecutive slices per animal ($n = 4$). The percentage of co-expressing cells was then calculated per image. The values from each image per animal were averaged to obtain a single number/animal and analyzed with a two-way ANOVA followed by the Holm-Sidak multiple comparisons' test (see Table 7). Significant ($P < 0.05$) effects of treatment within or between genotypes are indicated with an asterisk or a crosshatch, respectively. Scale bars = 50 μm. (For interpretation of the references to colour in this figure legend, the reader is referred to the web version of this article.)

Table 1

Reduced circadian outputs resulted from the long wavelength illumination.

Test	WT untreated	White Light	Short-λ enriched	Long-λ enriched	One way ANOVA
Masking (% reduction)	−3.0 ± 6.9 (*n* = 14)	−51.1 ± 5.2 (*n* = 8)	−51.0 ± 4.9 (*n* = 11)	**−13.6 ± 7.7$^{*,\#}$(n = 11)**	**$F_{(3,40)}$= 14.31; *P* < 0.0001**
Phase shift (min)	−3.7 ± 4.0 (n = 8)	−128.5 ± 12.5 (n = 14)	−117.2 ± 5.9 (n = 12)	**−26.4 ± 3.9$^{*,\#}$(n = 12)**	**$F_{(3,42)}$= 50.51; P < 0.0001**
# of c-Fos+ cells in the SCN	5.6 ± 0.4 (n = 4)	84.9 ± 5.8 (n = 4)	93.7 ± 6.2 (n = 4)	**18.8 ± 2.3 $^{*,\#}$ (n = 4)**	**$F_{(3,12)}$= 104.1; P < 0.0001**

WT mice were used to test whether the long wavelength (λ) light has a diminished impact on 3 traditional assays for light input to the circadian system. For masking, mice were exposed to light (10 lx, 60 min) from ZT 14 to 15. For phase shifts and induction of c-Fos expression, mice were held in constant darkness (DD) and exposed to light at CT 16 (10 lx, 15 min). Mice were euthanized 45 at CT 17 and the brains collected. The number of immunopositive cells in both the left and right SCN from two consecutive coronal sections per animal were averaged to obtain one number per animal. An equal number of male and female mice was used, and values are shown as the mean ± SEM. Data were evaluated by one way ANOVA followed by the Holm-Sidak Multiple comparisons' test. The asterisks indicate significant differences between white light and other 2 light wavelengths, and the crosshatches between the short- and long-λ. In this and subsequent tables, $P \leq 0.05$ was considered significant, and significant differences are shown in bold.

Table 2

Opn4^{DTA} mice were less affected by a short wavelength enriched DLaN.

	WT			*Opn4* ^{aDTA}		
	LD Control	**Short-λ DLaN**	**Statistic**	**LD Control**	**Short-λ DLaN**	**Statistic**
Masking (% reduction)	−8.9 ± 9.3	**−42.1 ± 7.3***	**$t_{(12)}$= 2.795; *P* = 0.016**	2.8 ± 10.4	10.0 ± 9.9	$t_{(12)}$ = −0.498; *P* = 0.628
Total activity (a.u./24 h)	3494.4 ± 538.6	**1589.8 ± 267.4***	**$t_{(8)}$= 5.408; *P* = 0.005**	2850.8 ± 889.9	2973.8 ± 801.9	$t_{(7)}$ = −0.368; *P* = 0.724
Power (% variation)	37.0 ± 3.7	**17.8 ± 1.7***	**$t_{(8)}$= 5.408; *P* = 0.005**	27.2 ± 1.9	28.9 ± 3.7	$t_{(7)}$ = −0.368; P = 0.724
Amplitude (Peak/trough)	316.7 ± 36.7	**140.8 ± 23.5***	**$t_{(8)}$= 4.031; *P* = 0.004**	271.1 ± 60.9	274.8 ± 67.0	$t_{(7)}$ = −0.040; *P* = 0.969
Activity in day (%)	19.0 ± 2.4	**26.6 ± 4.5***	**$t_{(8)}$= 5.408; *P* = 0.006**	27.2 ± 1.9	28.9 ± 2.8	$t_{(7)}$ = −0.368; P = 0.724
Fragmentation (bouts #)	9.0 ± 0.6	9.8 ± 0.7	$t_{(8)}$ = 0.826; *P* = 0.425	7.6 ± 0.8	8.4 ± 0.8	$U_{(7)}$ = 4.0; *P* = 0.190
Onset variability (min)	13.9 ± 1.3	25.7 ± 6.5	$t_{(8)}$ = −1.767; *P* = 0.057	14.8 ± 3.1	16.7 ± 3.3	$t_{(7)}$ = −0.401; *P* = 0.350

Light input to the circadian system is mediated by the ipRGC population that can be selectively ablated in a line of mice with the gene coding for melanopsin (OPN) expressing a component of the diphtheria toxin. We compared the impact of the short-λ enriched DLaN on the activity rhythms and social interaction behavioral test in WT and *Opn4*^{DTA} littermates. Both male and female mice were used. Values are shown as means ± SEM of n = 4–6 animals/genotype/light condition for the activity rhythms and n = 6–8 animals/genotype for the social interaction behavioral test. Because of the small sample size, the effects of the short wavelength enriched DLaN was analyzed only within the genotype with a paired *t*-test. This is a sensitive test to determine the possible impact of the DLaN treatment but does not allow us to compare between genotypes. For parameters that did not pass normality tests, the Mann Whitney rank-sum test was used, and the U values reported. *P* values <0.05 were considered significant. The asterisks indicate significant differences between LD and the short-λ enriched DLaN treatment within genotype. Significant differences are shown in bold. a.u. = arbitrary units.

Table 3

Long wavelength enriched illumination minimized DLaN disruption.

	WT			***Cntnap2* KO**			**Two-way ANOVA**	
	LD Control	**Short-λ DLaN**	**Long-λ DLaN**	**LD Control**	**Short λ DLaN**	**Long λ DLaN**	**Genotype**	**Treatment**
Total activity (a.u./24 h)	3003.9 ± 321	2114.3 ± 237	3443.3 ± 524	**1943.4 ± 135 #**	1639.4 ± 254	2145.6 ± 217	**$F_{(1,95)}$= 14.16; *P* < 0.001**	**$F_{(2,95)}$= 3.88; *P* = 0.024**
Power (% variance)	31.8 ± 1.1	**22.6 ± 1.0***	30.6 ± 2.2	**24.8 ± 1.2 #**	**19.3 ± 1.4***	28.9 ± 2.0	**$F_{(1,95)}$= 5.39; *P* = 0.022**	**$F_{(2,95)}$= 10.97; P < 0.001**
Amplitude (Peak/trough)	250.1 ± 29.6	**148.7 ± 1***	295.3 ± 45.9	**183.9 ± 15.9 #**	**132.1 ± 19.9***	212.1 ± 22.5	**$F_{(1,95)}$= 5.49; *P* = 0.018**	**$F_{(2,95)}$= 7.23; *P* = 0.001**
Activity in day (%)	18.7 ± 0.7	**26.0 ± 1.9***	19.6 ± 1.7	26.0 ± 2.0	32.3 ± 2.0	19.3 ± 1.6	$F_{(1,95)}$ = 2.80; *P* = 0.098	**$F_{(2,95)}$= 27.63; *P* < 0.001**
Onset variability (min)	18.2 ± 1.9	**33.44 ± 5***	25.0 ± 3.0	23.5 ± 2.0	**42.0 ± 6.1***	36.6 ± 2.9	**$F_{(1,95)}$= 10.27; *P* = 0.002**	**$F_{(2,95)}$= 16.10; *P* < 0.001**
Fragmentation (# bouts)	10.5 ± 0.9	10.7 ± 1.0	10.8 ± 2.0	11.6 ± 1.3	12.4 ± 1.5	11.6 ± 1.6	$F_{(1,95)}$ = 1.13; *P* = 0.29	$F_{(2,95)}$ = 0.07; *P* = 0.93
Social interaction (sec)	48.8 ± 6.2	**26.3 ± 6.8***	43.3 ± 9.6	**23.4 ± 3.4 #**	**8.6 ± 2.0***	16.9 ± 3.9	**$F_{(1,95)}$= 15.04; *P* < 0.001**	**$F_{(2,95)}$= 4.54; *P* = 0.013**
Grooming (sec)	13.4 ± 1.1	15.7 ± 2.0	10.1 ± 1.6	**31.2 ± 1.8 #**	**43.7 ± 2.8***	27.7 ± 2.5	**$F_{(1,151)}$= 149.14; *P* < 0.001**	**$F_{(2,151)}$= 11.51; *P* < 0.001**

Comparisons of age-matched WT and *Cntnap2* KO mice under LD or a DLaN regimen (n = 12–15/group). Values are shown as averages ± SEM. Data were analyzed with a two-way ANOVA using genotype and treatment as factors. The Holm-Sidak test for multiple comparisons was used when appropriate. The asterisks indicate significant differences between LD and DLaN treatments within genotype and the crosshatches between genotypes. Significant differences are shown in bold. a.u. = arbitrary units.

Table 4

Sex differences in WT and *Cntnap2* KO mice held in LD conditions.

	WT		***Cntnap2* KO**		**Two-way ANOVA**	
	Male LD	**Female LD**	**Male LD**	**Female LD**	**Genotype**	**Sex**
Measures	**n = 12–18**	**n = 11–18**	**n = 12–18**	**n = 12–18**		
Total activity (a.u./24 h)	2756.8 ± 327.6	3276.6 ± 429.8	2073.8 ± 213.8	**1812.9 ± 156.6** $^{\#}$	$\mathbf{F_{(1,46)} = 13.28; P < 0.001}$	$F_{(1,46)} = 0.19$; $P = 0.662$
Power (% variance)	31.9 ± 1.5	32.5 ± 1.5	**24.5 ± 1.4** $^{\#}$	**24.3 ± 1.7** $^{\#}$	$\mathbf{F_{(1,46)} = 19.92; P < 0.001}$	$F_{(1,46)} = 0.03$; $P = 0.873$
Amplitude (Peak/trough)	237.6 ± 29.2	251.4 ± 29.3	183.8 ± 14.9	**167.2 ± 18.2** $^{\#}$	$\mathbf{F_{(1,46)} = 8.54; P = 0.006}$	$F_{(1,46)} = 0.01$; $P = 0.951$
Social interaction (sec)	41.2 ± 6.4	56.0 ± 8.3	22.5 ± 5.2	22.5 ± 6.4	$\mathbf{F_{(1,47)} = 15.62; P < 0.001}$	$F_{(1,47)} = 1.26$; $P = 0.268$
Grooming (sec)	14.4 ± 1.6	12.3 ± 1.6	**35.8 ± 2.6** $^{*\#}$	**28.3 ± 2.0** $^{\#}$	$\mathbf{F_{(1,69)} = 82.34; P < 0.001}$	$\mathbf{F_{(1,69)} = 5.37; P = 0.024}$

Comparisons of age-matched male and female WT and *Cntnap2* KO mice held in LD. Values are shown as averages ± SEM. Data were analyzed with a two-way ANOVA using genotype and sex as factors. The Holm-Sidak test for multiple comparisons was used when appropriate. There were no significant interactions between genotype and sex, thus these values are not reported. The asterisks indicate significant differences between sexes and the crosshatches between genotypes. Significant differences are shown in bold. a.u. = arbitrary units.

Table 5

Sex differences in WT and *Cntnap2* KO mice under DLaN conditions.

	WT		*Cntnap2* KO		Two-way ANOVA	
	Male Short-λ DLaN	Female Short-λ DLaN	Male Short-λ DLaN	Female Short-λ DLaN	Genotype	Sex
Measures	**n = 6–8**	**n = 6–8**	**n = 6–11**	**n = 6–11**		
Total activity (a.u./24 h)	1755.3 ± 257.6	2473.4 ± 359.5	2152.9 ± 388.3	1892.6 ± 216.5	$F_{(1,23)}$ = 0.08; P = 0.773	$F_{(1,23)}$ = 0.53; P = 0.474
Power (% variance)	21.0 ± 1.0	24.2 ± 1.6	25.2 ± 1.8	22.0 ± 0.9	$F_{(1,23)}$ = 0.52; P = 0.479	$F_{(1,23)}$ = 0.01; P = 0.999
Amplitude (Peak/trough)	135.7 ± 19.5	161.7 ± 20.4	187.3 ± 25.7	156.8 ± 20.0	$F_{(1,23)}$ = 1.18; P = 0.291	$F_{(1,23)}$ = 0.01; P = 0.919
Social interaction (sec)	38.1 ± 11.3	17.8 ± 7.7	**7.9 ± 3.0** #	**11.0 ± 2.1** #	**$F_{(1,23)}$= 6.20; P = 0.022**	$F_{(1,23)}$ = 1.35; P = 0.259
Grooming (sec)	18.0 ± 2.7	13.42 ± 2.8	**44.4 ± 3.2** #	**44.9 ± 4.5** #	**$F_{(1,37)}$= 62.23; P < 0.001**	$F_{(1,37)}$ = 0.31; P = 0.578

Comparisons of age-matched male and female WT and *Cntnap2* KO mice held under a short-**λ** enriched DLaN for two weeks. Values are shown as averages ± SEM. Data were analyzed with a two-way ANOVA using genotype and sex as factors. There were no significant interactions between genotype and sex, thus, these are not reported. The Holm-Sidak test for multiple comparisons was used when appropriate. The crosshatches indicate significant differences between genotypes. Significant differences are shown in bold. a.u. = arbitrary units.

Table 6

Long wavelength enriched illumination minimized the DLaN-evoked cFos expression in several brain regions.

	WT			***Cntnap2* KO**			**Two-Way ANOVA**	
Brain region	**LD Control**	**Short λ DLaN**	**Long λ DLaN**	**LD Control**	**Short λ DLaN**	**Long λ DLaN**	**Genotype**	**Treatment**
pHb	30.1 ± 7.1	**55.4 ± 6.7***	34.7 ± 4.9	22.2 ± 1.6	**63.1 ± 8.1***	38.0 ± 6.4	$F_{(1,35)}$ = 0.047; P = 0.83	**$F_{(2,35)}$ = 71.94; P < 0.001**
BLA	170.2 ± 38.1	**235.1 ± 46.3***	160.2 ± 29.9	202.0 ± 42.0	**346.3 ± 27.1 *, #**	222.9 ± 25.8	**$F_{(1,35)}$ = 7.99; P = 0.008**	**$F_{(2,35)}$ = 5.99; P = 0.006**
SCN	4.6 ± 1.3	4.1 ± 0.8	4.6 ± 0.9	4.8 ± 1.5	3.3 ± 0.7	4.5 ± 0.7	$F_{(1,35)}$ = 0.09; P = 0.77	$F_{(2,35)}$ = 0.62; P = 0.54
PVN	28.4 ± 4.4	35.5 ± 4.8	29.6 ± 6.9	35.8 ± 7.6	35.5 ± 3.9	28.0 ± 7.0	$F_{(1,35)}$ = 0.19; P = 0.67	$F_{(2,35)}$ = 0.76; P = 0.48
LH	134.1 ± 42.0	133.6 ± 30.2	150.9 ± 28.2	140.1 ± 40.0	140.9 ± 12.5	121.7 ± 19.9	$F_{(1,35)}$ = 0.055; P = 0.82	$F_{(2,35)}$ < 0.001; P = 1.00

Number of cFos immunopositive cells in age-matched WT and *Cntnap2* KO mice under LD or a DLaN regimen (n = 6/group). Immunopositive cells were counted in both the left and right region of interest in two consecutive slice and the numbers averaged to obtain one value per animal. Values are shown as averages ± SEM. Data were analyzed with a two-way ANOVA using genotype and treatment as factors. The Holm-Sidak test for multiple comparisons was used when appropriate. There were no significant interactions between genotype and treatment. The asterisks indicate significant differences between LD and the short-λ enriched DLaN within genotype and the crosshatches between genotypes. SCN=Suprachiasmatic Nucleus; pHb = perihabenular nucleus; PVN=Periventricular Nucleus; LH = Lateral Hypothalamus; BLA = Basolateral Amygdala. Significant differences are shown in bold.

Table 7

Increased cFos expression in glutamatergic neurons in the BLA by the short wavelength enriched illumination.

	WT		***Cntnap2* KO**		**Two-Way ANOVA**		
	LD Control	**Short λ DLaN**	**LD Control**	**Short λ DLaN**	**Genotype**	**Treatment**	**Interaction**
vGlut2-ZsGreen1 cells (#)	43.4 ± 3.1	47.2 ± 2.2	45.2 ± 2.3	**33.2 ± 1.0** *,#	**$F_{(1,12)}$ = 7.225; P = 0.019**	$F_{(1,12)}$ = 3.162; P < 0.1007	$F_{(1,12)}$ = 11.90; P = 0.005
vGlut2-ZsGreen1-cFos positive (#)	9.1 ± 0.7	**18.9 ± 1.4***	8.8 ± 1.8	**17.7 ± 1.3***	$F_{(1,12)}$ = 0.322; P = 0.581	**$F_{(1,12)}$ = 45.78; P < 0.0001**	$F_{(1, 12)}$ = 0.111; P = 0.745
% co-expression	21.0 ± 1.0	**40.5 ± 4.0***	19.7 ± 4.6	**53.6 ± 5.5***	$F_{(1,12)}$ = 2.017; P = 0.181	**$F_{(1, 12)}$ = 41.68; P < 0.0001**	$F_{(1,12)}$ = 2.998; P = 0.109

Comparisons of vGlut2-ZsGreen1-cFos positive cells in the BLA of WT and *Cntnap2* KO mice under LD or a DLaN regimen (n = 4/group) showed a marked increase in the percentage of cFos positive cells in the mutants exposed to the short-λ enriched DLaN. The number of vGlut2-ZsGreen1 expressing neurons and, among these neurons, the number of cFos positive cells was determined in 4 to 7 images per animal. The percentage of co-expressing cells was then calculated per image. These values were averaged to obtain a single number per animal. Data are shown as the average ± SEM and were analyzed with a two-way ANOVA using genotype and treatment as factors followed by the Holm-Sidak test for multiple comparisons. The asterisks indicate significant differences between LD and the short-λ enriched DLaN treatment within genotype and the crosshatches between genotypes. Significant differences are shown in bold.